`wavecontrol`: A program for the Control and Stabilization of waves. Manual.

Contributors:

C. Castro[1], M. Cea[2] , S. Micu[3], A. Münch[4], M. Negreanu[5] and E. Zuazua[6]

[1]ETSI de Caminos, Canales y Puertos, Universidad Politécnica de Madrid, 28040 Madrid, Spain (`ccastro@caminos.upm.es`)

[2]Departamento de Matemáticas, Facultad de Ciencias, Universidad Autónoma de Madrid, 28049 Madrid (`miguel.cea@uam.es`)

[3]Facultatea de Matematica-Informatica, Universitatea din Craiova, 1100, Romania (`sd_micu@yahoo.com`)

[4]Laboratoire de Mathématiques de Besançon, UMR CNRS 6623, Université de Franche-Comte, 16 route de Gray, 25030 Besançon cedex, France (`arnaud.munch@math.univ-fcomte.fr`)

[5]Departamento de Álgebra, Facultad de Informática, Universidad Complutense de Madrid, 28040 Madrid (`mihaela_negreanu@mat.ucm.es`)

[6]Departamento de Matemáticas, Facultad de Ciencias, Universidad Autónoma de Madrid, 28049 Madrid (`enrique.zuazua@uam.es`)

Contents

Introduction

`Wavecontrol` is a guide user interface (GUI) programmed with MATLAB that allows to solve numerically several control and stabilization problems for the wave equation. The program offers to the user a number of solvers with different numerical methods for each problem, and the possibility to choose several data by means of a graphic interface.

More precisely, `wavecontrol` performs numerical solutions for the following problems:

- The boundary control of the 1-D wave equation when acting at one of the extremities with finite differences, the finite element method and a particular mixed finite element method (that we describe below).
- The boundary control of a 2-D wave equation in a square, with the control located at two adjacent sides, with finite differences and bi-grid methods.
- The stabilization of the 1-D wave equation in an interval with a damping acting on an internal subset, discretized with finite differences and numerical viscosity.
- The stabilization of the 2-D wave equation in a square with a damping acting on an internal set, discretized with finite differences and numerical viscosity.

In all these problems the user can choose, among other parameters, the initial data to be controlled or stabilized.

This manual contains a detailed description of the above problems, the numerical algorithms used to compute the solution and a guide to use the program `wavecontrol` illustrated with several examples.

This document is divided in three parts. In the first part we introduce the problems, describe the main results known and discuss the numerical issues to approximate the solutions. The second part is devoted to describe the program with a short user guide. Finally, in the last part we present some significant examples which illustrate the main features of the implemented numerical methods.

Chapter 1

Theoretical results

1.1 The exact boundary control problem

We consider the exact boundary controllability problem of the wave equation in a bounded domain $\Omega \subset R^d$ $(d = 1, 2)$. We assume that the control acts in one part of the boundary of Ω, $\Gamma \subset \partial\Omega$. The formulation of the problem is as follows: given $T > 0$ and $(u^0, u^1) \in L^2(\Omega) \times H^{-1}(\Omega)$, to find a control function $v \in L^2(\Gamma \times (0, T))$ such that the solution of the system:

$$\begin{cases} u_{tt} - \Delta u = 0, & x \in \Omega, \quad 0 < t < T, \\ u(x,t) = 0, & x \in \partial\Omega \backslash \Gamma, \quad 0 < t < T, \\ u(x,t) = v(x,t), & x \in \Gamma, \quad 0 < t < T, \\ u(x,0) = u^0(x), \qquad u_t(x,0) = u^1(x), & x \in \Omega \end{cases} \tag{1.1}$$

satisfies

$$u(x,T) = u_t(x,T) = 0, \qquad x \in \Omega, \tag{1.2}$$

($_t = \partial/\partial t$ denotes partial derivation with respect to time).

It is well-known that, there are two main necessary conditions for this problem to have a positive answer: (i) T must be large enough and (ii) Γ must satisfy the so-called Geometrical Control Condition (GCC).

Roughly speaking, condition (ii) says that there exists a uniform time $T > 0$ such that any "ray", starting at any point $x \in \Omega$ and in any direction, has to meet ω in time T. In particular, this geometric condition is fulfilled when Γ is the whole boundary of Ω, the time being the diameter of Ω. If this condition is not satisfied, it would be possible to construct some initial data, with energy trapped in some rays that never meet Γ. This initial data will never be controlled from Γ.

Condition (i) comes from the fact that waves propagates at finite velocity. In fact, for the constant coefficients wave equation, the *waves* propagate along characteristics with velocity one. On the other hand, the control $v(x,t)$ is located at one part of the boundary of the domain Γ and it only takes care of the *waves* arriving there at time t. Thus, in order to capture all possible *waves* coming from the initial data it is necessary to wait for some minimal time T_{min}. If Γ is the whole boundary of Ω then T_{min} is the diameter of Ω.

Assuming that both (i) and (ii) are satisfied, the above control problem has at least one solution $v \in L^2(\Gamma \times (0, T))$ (see for example [3]). In general, the solution of the above control problem is not unique. However, among all possible controls it is possible to select the one of minimal L^2-norm. This control is unique and can be characterized by the so-called HUM method introduced by J.-L. Lions ([13]).

Even if the existence and uniqueness of the HUM control is well-understood, its numerical approximation is not an easy problem. We briefly explain why. In general, any discrete dynamics associated to the wave equation generates spurious high-frequency oscillations that do not exist at the continuous level. Moreover, a numerical dispersion phenomenon appears and the velocity of propagation of some high frequency numerical waves may possibly converge to zero when the mesh

size h does. In this case, the controllability property for the discrete system will not be uniform, as $h \to 0$, for a fixed time T and, consequently, there will be initial data (even very regular ones) for which the corresponding controls of the discrete model will diverge in the L^2-norm as h tends to zero. For example, this is the case when we consider a semi-discretization of the wave equation with the classical finite differences or finite element method (see [11] for a detailed analysis of the 1-D case and [24] for the 2-D case, in the context of the dual observability problem).

In [11] it was shown that, after filtering the high frequency modes, an uniform observability inequality for the adjoint system holds. This is equivalent with the uniform controllability of the projection of the solutions over the space generated by the remaining eigenmodes. Observe that the dimension of this space tends to infinity as the step size h goes to zero and that, in the limit, we would obtain the control of the continuous system. However, in practice these projection methods are not very efficient.

In [14] the problem with finite difference approximations was considered again. It was proved that, if the high frequency modes of the *discrete initial data* are filtered out in an appropriate manner (or if the initial data are sufficiently regular), there are controls of the semi-discrete model which converge to a control of the continuous wave equation. This is one of the ways of taking care of the spurious high frequency oscillations that the numerical method introduces. Note that in this case the uniform controllability of the entire discrete solutions is ensured and not only that of the projections, as in [11]. Moreover, it was also shown that the norm of the discrete HUM controls may increase exponentially with the number of points in the mesh if no filtering is applied.

From a numerical point of view, several techniques have been proposed as possible cures of the high frequency spurious oscillations. For example, in [8] a Tychonoff regularization procedure was successfully implemented. Roughly speaking, this method introduces an additional control, tending to zero with the mesh size, but acting on the interior of the domain. Other proposed numerical techniques are multi-grid (see [8] and [6]) and mixed finite element methods (see [9]).

Finally in [4] and [5] a mixed finite elements method is considered for 1-D and 2-D wave equations respectively. The main advantage of this method is that it is uniformly controllable as the discretization parameter h goes to zero and allows to construct a convergence sequence of approximate controls (as $h \to 0$) without filtering. It consists in a different space discretization scheme of the wave equation derived from a *mixed finite element method*, which is based on different discretizations for the position and velocity. More precisely, while the classical first order splines are used for the former, discontinuous elements approximate the latter. This method is different to the one used in [9] where u and ∇u are approximated in different finite dimensional spaces.

To our knowledge, this mixed finite element approach was used by the first time in the context of the wave equation in [2], in order to obtain a uniform decay rate of the energy associated to the semi-discrete wave equation by a boundary dissipation. Later on, in [12], a rigorous analysis of the convergence and error estimates of the scheme (without control) where given.

To solve the controllability problem stated above we follow the HUM approach introduced by J.-L. Lions in [13]. Its main advantage is that the control is characterized by a variational formulation that can be easily implemented by a conjugate gradient algorithm, as we show below.

In the next two subsection we detail the HUM method for the controllability of the 1-D wave equation in a segment and the 2-D one in a square domain.

1.1.1 The $1-D$ control problem. HUM approach

We consider the controllability problem for the 1-D wave equation on an interval $(a,b) \subset R$, with the control located at the extremity $x = b$. The formulation of the problem is as follows: given $T > 0$ and $(u^0, u^1) \in L^2(a,b) \times H^{-1}(a,b)$, to find a control function $v \in L^2(0,T)$ such that the solution of the system:

$$\begin{cases} u_{tt} - u_{xx} = 0, & a < x < b, \quad 0 < t < T, \\ u(a,t) = 0, \quad u(b,t) = v(t), & 0 < t < T, \\ u(x,0) = u^0(x), \qquad u_t(x,0) = u^1(x), & a < x < b \end{cases} \tag{1.3}$$

satisfies

$$u(x,T) = u_t(x,T) = 0, \qquad x \in (a,b). \tag{1.4}$$

($_t = \partial/\partial t$ and $_x = \partial/\partial x$ denote partial derivation with respect to time and space, respectively).

It is well-known that, when $T \geq 2(b-a)$, this control problem has at least one solution $v \in L^2(0,T)$ (see for example [13]). We solve this problem using HUM.

We introduce the homogeneous adjoint system

$$\begin{cases} \phi_{tt} - \phi_{xx} = 0, & a < x < b, \quad 0 < t < T, \\ \phi(a,t) = \phi(b,t) = 0, & 0 < t < T, \\ \phi(x,0) = \phi^0(x), \qquad \phi_t(x,0) = \phi^1(x), & a < x < b. \end{cases} \tag{1.5}$$

Let us denote by $E = H_0^1(a,b) \times L^2(a,b)$ the energy space of initial states for this homogeneous wave equation. Let further $E' = H^{-1}(a,b) \times L^2(a,b)$ be the dual space of E, and define the operator

$$\Lambda : E \to E'$$

as follows:

- Given $e = \left\{\phi^0, \phi^1\right\} \in E$, let ϕ be the solution of the uncontrolled wave equation (1.5) with initial state $(\phi^0(x), \phi^1(x)) = e$.
- Let ψ be the solution of the backward controlled system from $t = T$ to $t = 0$ with boundary data $\partial\phi(b,t)/\partial x$ at the end point $x = b$:

$$\begin{cases} \psi_{tt} - \psi_{xx} = 0, & a < x < b, \quad 0 < t < T, \\ \psi(a,t) = 0 \qquad \psi(b,t) = \dfrac{\partial\phi(b,t)}{\partial x}, & 0 < t < T, \\ \psi(x,T) = \psi_t(x,T) = 0, & a < x < b, \end{cases} \tag{1.6}$$

- Set

$$\Lambda\, e = \{\psi_t(0), -\psi(0)\}\,. \tag{1.7}$$

It is proved in [13] that Λ is a *linear* and *continuous* operator from E into E'. Moreover, if T is *sufficiently large* ($T \geq T_{\min} = 2(b-a)$), then Λ is an *isomorphism* from E onto E'.

Now, given (u^0, u^1) the initial data to be controlled, let $\hat{e} \in E$ be such that

$$\Lambda\, \hat{e} = \left\{u^1, -u^0\right\}. \tag{1.8}$$

Then

$$v(t) = \partial_x \hat{\phi}(b,t), \tag{1.9}$$

where $\hat{\phi}$ is the solution of (1.5) corresponding to $\hat{e}$, is a solution of the control problem.

Remark 1. *1. The solution $\hat{e} = (\hat{\phi}^0, \hat{\phi}^1) \in H_0^1(a,b) \times L^2(a,b)$, of (1.8) can be also characterized as the unique minimizer of the functional*

$$J(\phi^0, \phi^1) = \frac{1}{2}\int_0^T \mid \partial_x \phi(b,t) \mid^2 dt + \int_a^b u^0 \phi^1 - < u^1, \phi^0 >_{-1,1},$$

in the space $H_0^1(a,b) \times L^2(a,b)$. Here $\phi(x,t)$ is the solution of (1.5) with initial data (ϕ^0, ϕ^1).

2. The control $v(t)$ in (1.9) is not the unique solution of the control problem (1.3)-(1.4). However, it is possible to prove that the solution in (1.9) is the one with minimal $L^2(0,T)$-norm. In fact, the linear problem (1.8) is in duality with the following minimization one:

$$\min_{U} \int_0^T v^2 dt, \tag{1.10}$$

where the set of admissible controls is given by

$$\mathcal{U} = \{v \in L^2(0,T) \mid \textit{ the solution } u \textit{ of (1.3) satisfies (1.4)}\}.$$

Thus, the HUM control is the unique *solution of the minimization problem (1.10) (see [13], [6] for more details). In other words, HUM provides the control with minimal* $L^2(0,T)$*-norm.*

1.1.2 The $2-d$ control problem

Here we consider the 2-D version of the above problem in a square domain $\Omega = (a,b)\times(a,b) \subset \mathbb{R}^2$. We assume that the control is located at two adjacent sides of the boundary of Ω, $\partial\Omega$, that we denote by $\Gamma_1 = \{(x_1,b) \cup (b,x_2), \text{ with } a \le x_1, x_2 \le b\} \subset \partial\Omega$.

The control problem reads as follows: given $T > 0$ and the initial data $(u^0, u^1) \in L^2(\Omega) \times H^{-1}(\Omega)$, to find $v(x,t) \in L^2(\Gamma_1 \times (0,T))$ such that the solution u of the constant coefficient $2-d$ wave system (Δ is the Laplacian in the space variable $x = (x_1, x_2) \in \Omega$):

$$\begin{cases} u_{tt} - \Delta u = 0, & \text{in} \quad \Omega \times (0,T), \\ u(x,t) = 0 \quad \text{on } \Gamma_0 = \partial\Omega \backslash \Gamma_1, \quad u(x,t) = v(x,t) \quad \text{on } \Gamma_1, & 0 < t < T, \\ u(x,0) = u^0(x), \qquad u_t(x,0) = u^1(x), & \text{in} \quad \Omega. \end{cases} \tag{1.11}$$

satisfies

$$u(x,T) = u_t(x,T) = 0, \quad x \in \Omega.$$

To solve this problem by HUM we introduce the corresponding homogeneous adjoint system

$$\begin{cases} \phi_{tt} - \Delta\phi = 0, & \text{in} \quad \Omega \times (0,T), \\ \phi(x,t) = 0, & \text{on} \quad \partial\Omega \times (0,T), \\ \phi(x,0) = \phi^0(x), \qquad \phi_t(x,0) = \phi^1(x), & \text{in} \quad \Omega. \end{cases} \tag{1.12}$$

Let us denote by $E = H_0^1(\Omega) \times L^2(\Omega)$ the space of initial states for the homogeneous wave equation. Let further $E' = H^{-1}(\Omega) \times L^2(\Omega)$ be the dual space of E, and define the operator

$$\Lambda : E \to E'$$

as follows:

- Given $e = \{\phi^0, \phi^1\} \in E$, let ϕ be the solution of the uncontrolled wave equation (1.12) with initial state $(\phi^0(x), \phi^1(x)) = e$.
- Let ψ be the solution of the backward controlled system from $t = T$ to $t = 0$ with boundary data $\partial\phi(x,t)/\partial n$ on Γ_1

$$\begin{cases} \psi_{tt} - \Delta\psi = 0, & \text{in} \quad \Omega \times (0,T), \\ \psi(x,t) = 0 \quad \text{on } \Gamma_0, \quad \psi(x,t) = \dfrac{\partial\phi(x,t)}{\partial n} \quad \text{on } \Gamma_1, & 0 < t < T, \\ \psi(x,T) = \psi_t(x,T) = 0, & \text{in} \quad \Omega, \end{cases} \tag{1.13}$$

- Define $\Lambda\, e$ by

$$\Lambda\, e = \{\psi_t(0), -\psi(0)\}. \tag{1.14}$$

Given (u^0, u^1), the initial data to be controlled, let $\hat{e}$ be such that

$$\Lambda\, \hat{e} = \left\{u^1, -u^0\right\}. \tag{1.15}$$

Then

$$v(x,t) = \frac{\partial \hat{\phi}(x,t)}{\partial n}, \tag{1.16}$$

where $\hat{\phi}$ is the solution of (1.12) corresponding to the initial data $\hat{e} = (\hat{\phi}^0, \hat{\phi}^1)$, is a solution to the control problem.

Remark 2. *1. The initial data $(\hat{\phi}^0, \hat{\phi}^1) \in H_0^1(\Omega) \times L^2(\Omega)$, can be also characterized as the unique minimizer of the functional*

$$J(\phi^0, \phi^1) = \frac{1}{2}\int_0^T \int_{\Gamma_1} \left|\frac{\partial \phi(x,t)}{\partial n}\right|^2 d\sigma dt + \int_\Omega u^0 \phi^1 dx - < u^1, \phi^0 >_{-1,1}$$

in the space $H_0^1(\Omega) \times L^2(\Omega)$.

2. In general the above control problem has many different solutions. The solution $v \in L^2(\Gamma_1, (0,T))$ in (1.16) is the one with minimal L^2-norm (the so-called HUM control).

1.2 Stabilization of the wave equation

We study now the stabilization problem for the wave equation. We focus only on the 2-D case.

Let $\Omega \subset \mathbb{R}^2$ be a bounded domain. Consider the damped wave equation

$$\begin{cases} u_{tt} - \Delta u + c1_\omega u_t = 0, & \text{in} \quad \Omega \times (0,\infty), \\ u(x,t) = 0, & \text{on } \partial\Omega, \quad t > 0, \\ u(x,0) = u^0(x), \qquad u_t(x,0) = u^1(x), & \text{in } \Omega, \end{cases} \tag{1.17}$$

where $\omega \subset \Omega$ is a sub-domain of Ω, c is a positive constant and 1_ω denotes the characteristic function of the set ω where the damping term is effective.

The energy of (1.17) is defined as

$$E(t) = \frac{1}{2}\int_\Omega \left[|u_t(x,t)|^2 + |\nabla u(x,t)|^2\right] dx. \tag{1.18}$$

Given ω and c, we say that the energy *decays exponentially* if there exist constants $C > 0$ and $\gamma > 0$, independent of the solution u, such that

$$E(t) \le Ce^{-\gamma t} E(0) \tag{1.19}$$

holds for every finite energy solution of damped wave equation (1.17).

It is known that, in order to have the exponential decay the sub-domain ω, where the damping is effective, must satisfy the so-called Geometric Control Condition (GCC) (see [23], [3]). Roughly speaking, this condition says that there exists a uniform time $T > 0$ such that any "ray", starting at any point $x \in \Omega$ and in any direction, has to meet ω in time T. In particular, this geometric condition is fulfilled when ω is a neighborhood of the boundary of Ω, the time being the diameter of $\Omega \backslash \omega$.

Assume that ω satisfies the GCC. When discretizing system (1.17) it is natural to analyze whether the decay rate of the energy remains uniform with respect to the mesh size. The answer is in general negative. Indeed, due to spurious high frequency oscillations, the decay rate fails to be uniform, for instance, for the classical finite difference semi-discrete approximation of the wave equation. The uniformity of the exponential decay rate can be reestablished if we add an internal viscous damping term to the equation (see [23]).

In our programs we consider the particular case in which $\Omega = (a,b) \times (a,b)$ is a square domain and ω is a neighborhood of two adjacent sides.

1.3 Discretization procedures

We divide this section in four subsections. In the first two subsections we discuss the space semi-discretization of the 1-D, and 2-d wave equations respectively, that are needed for the boundary controllability problems. In the third subsection we deal with the space discretization of the damped wave equation that we use to approximate the stabilization problem, both in 1-D and 2-d. Finally, in the last subsection we focus on the time discretization method used to approximate any general semi-discrete second order system obtained by a semidiscretization of the wave equation.

1.3.1 Space discretization procedures for the $1-D$ wave equation

We introduce a uniform mesh of the space interval (a,b) with step $h=(b-a)/(n+1)$, where n is the number of internal points or *nodes*.

The wave equations (1.5) and (1.6) are then replaced by semi-discrete systems of the form

$$MU''+KU=F,$$

where M is the mass matrix, K is the stiffness matrix, F is the vector of applied forces and $U=(U_1,\cdots,U_n)^T$ is the displacement vector at the nodes. These semi-discrete systems are then solved by the Newmark method.

Thus the semi-discrete version of (1.5) is given by:

$$M\Phi''+K\Phi=0,\qquad \Phi(0)=\Phi^0,\qquad \Phi'(0)=\Phi^1,$$

while the corresponding semi-discrete version of (1.6) has a nonzero force F coming from the value of the solution at the boundary:

$$M\Psi''+K\Psi=F,\qquad \Psi(T)=\Psi'(T)=0.$$

The following choices of K and M are considered:

$$K=-\Delta_h:=\frac{1}{h^2}\begin{bmatrix} 2 & -1 & 0 & \cdots & 0 & 0 & 0\\ -1 & 2 & -1 & \cdots & 0 & 0 & 0\\ 0 & -1 & 2 & \cdots & 0 & 0 & 0\\ \vdots & \vdots & \vdots & \ddots & \vdots & & \\ 0 & 0 & 0 & \cdots & 2 & -1 & 0\\ 0 & 0 & 0 & \cdots & -1 & 2 & -1\\ 0 & 0 & 0 & \cdots & 0 & -1 & 2 \end{bmatrix},\qquad M=I+rh^2\Delta_h. \tag{1.20}$$

The parameter r allows to choose three particularly interesting models:

1. $r=0$. In this case $M=I$ and we obtain the finite difference method.
2. $r=1/6$. In this case M is known as *consistent mass matrix* and the system corresponds to the classical finite element method of order 1.
3. $r=1/4$. In this case M is the matrix associated to the mixed finite element method in which the position is approximated with piecewise linear functions while the velocity is approximated with piecewise constant functions (see [4]).

Other choices of r are also possible. In particular $r=1/12$ provides the *higher order mass matrix* (see [10] for more details).

It is known that, for some initial data, the controls obtained when discretizing the wave equation with finite differences ($r=0$) or finite elements ($r=1/6$) may diverge, as the mesh size h goes to zero, even if the continuous control exists (see [11] and [24] and the references therein). This is due to the fact that the semi-discrete dynamics introduces high frequency dispersion phenomena

and the velocity of propagation of some high frequency discrete waves vanishes, as $h \to 0$. This is in contrast with the continuous wave equation for which the velocity of propagation of all waves is one (see the Appendix below).

To overcome this difficulty there are several possibilities:

1. A mixed finite element approximation which corresponds to consider $r = 1/4$. Then the dispersion phenomenon for the high frequencies is completely different than in the previous cases and the velocity of propagation of the high frequency discrete waves becomes infinity, as $h \to 0$. Thus, the minimal velocity of propagation of waves in this semi-discrete system is the same as in the continuous case (see [4] for details).

2. Filtering techniques. Briefly, it consists in removing from the solution of the wave equation the part which corresponds to the numerical high frequencies. An efficient way to do that is to implement a bigrid algorithm (see [8] and our discussion on the conjugate gradient algorithm below).

3. A Tychonov regularization technique (see [8] for details).

1.3.2 Space discretization procedures for the $2-d$ wave equation

We introduce a uniform mesh of the space square $(a,b)\times(a,b)$ by considering a uniform mesh in (a,b), for both variables, with step $h=(b-a)/(n+1)$. The n^2 interior nodes are then numbered from left to right and from the lower to the upper part of the square.

The wave equations (1.12) and (1.13) are then replaced by a semi-discrete system of the form

$$MU_{tt} + KU = F, \tag{1.21}$$

where M is the $2-D$ mass matrix, K is the $2-D$ stiffness matrix, F is the vector of applied forces and $U=(U_1,\cdot,U_{n^2})$ is the displacement vector at each node.

Depending on the method chosen to approximate the wave equation we have several possibilities for the matrixes M and K.

Here we only consider the following choices:

$$K=-\Delta_h=\frac{1}{h^2}\begin{pmatrix} A & -I & & & \\ -I & A & -I & & (0) \\ & -I & \ddots & \ddots & \\ & & \ddots & \ddots & -I \\ & (0) & & -I & A \end{pmatrix}_{n^2\times n^2}, M=I_{n^2\times n^2}, \tag{1.22}$$

where

$$A=\begin{pmatrix} 4 & -1 & & & \\ -1 & 4 & -1 & & (0) \\ & -1 & \ddots & \ddots & \\ & & \ddots & \ddots & -1 \\ & (0) & & -1 & 4 \end{pmatrix}_{n\times n}. \tag{1.23}$$

As in the 1-D case, due to the dispersion phenomenon of the semi-discrete model, the controls obtained when discretizing the wave equation with this approximation may diverge as the mesh size h goes to zero (see the Appendix below).

There are several possibilities to deal with this problem:

1. A mixed finite element approximation in which the elements are squares and the position u and velocity u_t are approximated in different finite dimensional spaces. More precisely, while the classical first order splines are used for the former, discontinuous elements approximate the latter (see Figure 1). The dispersion associated to this scheme makes high frequencies to travel faster than in the continuous wave equation (see [5] and the Appendix below).

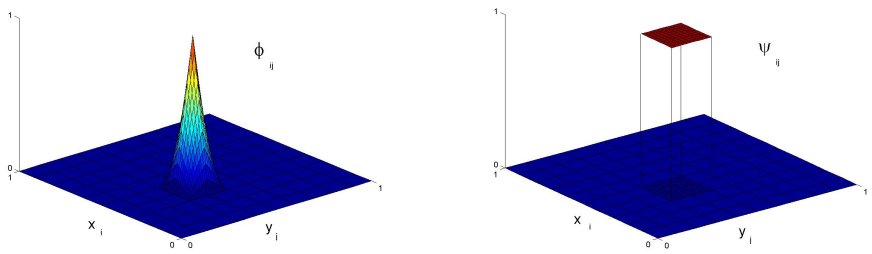

Figure 1.1: Base functions to approximate the position u (left) and the velocity u_t (right) in the mixed finite element method.

2. Filtering techniques (bigrid algorithm). (see [8] and our discussion on the conjugate gradient algorithm below).

3. A Tychonov regularization technique (see [8] for details).

1.3.3 Space discretization procedures for the stabilization of the wave equation

The damped wave equation (1.17) can be also approximated by the semi-discrete system

$$U'' + CU' + KU = 0, \qquad U(0) = U^0, \qquad U'(0) = U^1, \tag{1.24}$$

where U is the displacement vector at the nodes and K is the rigidity matrix which depends on the dimension of the problem as specified in the previous section (see (1.20) in the 1-D case and (1.22) in the 2-d one).

The matrix C is given by

$$C = C_1 - \nu(h)\Delta_h, \tag{1.25}$$

where $\nu(h)$ is a numerical viscosity coefficient such that $\nu(h) \to 0$ as $h \to 0$, and C_1 is an approximation of the characteristic function of the set ω, where the damping is located. In the 2-d case, C_1 is given by

$$C_1 = C \begin{bmatrix} \delta_1 & 0 & 0 & \cdots & 0 & 0 & 0 \\ 0 & \delta_2 & 0 & \cdots & 0 & 0 & 0 \\ 0 & 0 & \delta_3 & \cdots & 0 & 0 & 0 \\ \vdots & \vdots & \vdots & \ddots & \vdots & & \\ 0 & 0 & 0 & \cdots & \delta_{n^2-2} & 0 & 0 \\ 0 & 0 & 0 & \cdots & 0 & \delta_{n^2-1} & 0 \\ 0 & 0 & 0 & \cdots & 0 & 0 & \delta_{n^2} \end{bmatrix}, \qquad \delta_i = \begin{cases} 1 \text{ if } x_i \in \omega \\ 0 \text{ otherwise} \end{cases} \tag{1.26}$$

and an analogous expression is taken for the 1-D case.

The numerical viscosity term in (1.25) is necessary to recover the exponential decay rate of the continuous wave equation as $h \to 0$. In fact, as it was proved in [23], the exponential decay for system (1.24) remains uniform as $h \to 0$ provided one chooses the numerical viscosity term $\nu(h)$ of a suitable order, the optimal one being $\nu(h) \sim h^2$.

The semi-discrete scheme (1.24)-(1.26) may also be viewed as the semi-discretization of the viscoelastic wave equation with damping,

$$u_{tt} - \Delta u + (c - \nu(h)\Delta u)1_\omega u_t = 0. \tag{1.27}$$

1.3.4 Time discretization

The above semi-discrete systems can be written in a general form as follows

$$MU'' + CU' + KU = F, \tag{1.28}$$

where M is the mass matrix, C is the viscous damping matrix, K is the stiffness matrix, F is the vector of applied forces and U, U', U'' are the displacement, velocity and acceleration vectors, respectively. We take M, C, K to be symmetric; M is positive-definite, and C and K are positive-semidefinite.

The initial-value problem for (1.28) consists in finding a displacement, $U = U(t)$, satisfying (1.28) and the given initial data:

$$U(0) = U_0, \qquad U'(0) = V_0. \tag{1.29}$$

One of the most widely used family of methods for solving (1.28)-(1.29) is the *Newmark* one ([18]).

Let $0 = t_0 < t_1 < ... < t_N < t_{N+1} = T$ be a uniform partition of the time interval $(0, T)$ with step $\Delta t = T/(N + 1)$. Let also U_j, V_j and A_j be the approximations of U, U' and U'' at time $t = t_j$, respectively. Newmark methods are obtained substituting (1.28)-(1.29) by the following system of equations:

$$MA_{j+1} + CV_{j+1} + KU_{j+1} = F_{j+1}, \tag{1.30}$$

$$U_{j+1} = U_j + \Delta t V_j + \frac{\Delta t^2}{2}\left[(1 - 2\beta)A_j + 2\beta A_{j+1}\right], \tag{1.31}$$

$$V_{j+1} = V_j + \Delta t\left[(1 - \gamma)A_j + \gamma A_{j+1}\right], \tag{1.32}$$

$$U_0 = U(0), \qquad V_0 = U'(0), \qquad MA_0 = F_0 - KU_0. \tag{1.33}$$

Equation (1.30) is simply the equation of motion in terms of the approximate solution and (1.31) and (1.32) are finite difference formulas for the evolution of the displacements and velocities which are clearly inspired in the Taylor expansion. Equations (1.30)–(1.32) may be thought as three equations for determining the three unknowns U_{j+1}, V_{j+1} and A_{j+1}, assuming that U_j, V_j and A_j are known from the previous step's calculations.

The parameters β and γ determine the stability and accuracy characteristics of the algorithm under consideration (see for example [22] for details). We only comment two particular cases that are the most usual ones:

1. Central difference, $\beta = 0$ and $\gamma = 1/2$. It is a second-order explicit method (strictly speaking, M and C need to be diagonal for the central-difference method to be explicit (see [18])). The stability criterium is known as the Courant-Friederichs-Lewy condition (CFL) which reads

$$\frac{\Delta t}{h} \leq \frac{1}{c_h}, \tag{1.34}$$

   where c_h is the maximum velocity of propagation of the space semi-discrete model. In general explicit schemes are preferable since they are easier to implement and less time consuming.

2. Trapezoidal rule, $\beta = 1/4$ and $\gamma = 1/2$. It is second-order too but implicit. It also has the following two important properties: it is energy-conserving (see [22]) and unconditionally stable, i.e. it is stable for any choice of the Courant number $\mu = \Delta t/h$.

In the particular context of the controllability problem the natural choice for the time discretization scheme depends on the chosen scheme for the discretization in space:

1. Central difference in space. This is the simplest discretization procedure. The central difference in time with $\Delta t = h$ will produce a exact scheme, i.e. the exact solution of the wave equation at the nodes. This is a very special situation that appears only for the 1-D wave equation. The dispersion of the semi-discrete scheme is corrected by the time discretization and a non-dispersive scheme is obtained (see the Appendix below). In this case, the control algorithm will converge. Other choices of the ratio $\Delta t/h$ will produce dispersion of the high frequencies and lack of convergence of the control algorithm, for some initial data.

2. Mixed finite element approximation in space. In this case, the velocity of propagation of the high frequency numerical waves becomes large, as $h \to 0$. Thus, an easy computation shows that, for the central difference scheme, the CFL condition (1.34) requires

$$\begin{aligned} \Delta t &\leq Ch^2, \quad \text{in 1-D,} \\ \Delta t &\leq Ch^3, \quad \text{in 2-D.} \end{aligned}$$

   Therefore, it is natural to try the implicit scheme. In this case, the stability is not a problem but the velocity of propagation of high frequencies may possibly become zero as $h \to 0$. A detailed analysis show that, in this case, the velocity of propagation of the high frequency numerical waves is uniformly (in h) bounded from below under the conditions,

$$\begin{aligned} \Delta t &\leq Ch, \quad \text{in 1-D,} \\ \Delta t &\leq Ch^{3/2}, \quad \text{in 2-D.} \end{aligned}$$

3. Filtering techniques (bi-grid algorithm). In this case the simplest central difference is preferable since the high frequencies are filtered and it is stable under the natural condition $\Delta t \leq Ch$, for some $C > 0$.

1.4 Conjugate gradient implementation of HUM

The outline of this section is as follows: after a short recapitulation of the conjugate gradient-algorithms (*cg-algorithms*) for the numerical solution of Linear Variational Problems we specify its application to the boundary control of the wave equation.

1.4.1 Conjugate Gradient Algorithm. Generalities.

The original control problem may be transformed to that of solving the equation $\Lambda e = f$, which is a particular case of the abstract linear variational problem,

$$u \in V, \qquad a(u,v) = L(v), \qquad \forall v \in V, \tag{1.35}$$

where in (1.35):

1. V is a real Hilbert space for the scalar product $(\cdot,\cdot)$ and the corresponding norm $\|\cdot\|$.
2. $a : V \times V \to \mathbb{R}$ is bilinear, symmetric, continuous and V-elliptic.
3. $L : V \to \mathbb{R}$ is linear and continuous.

With the above hypotheses, problem (1.35) has a unique solution, which can be computed by the following *Conjugate Gradient* algorithm (see [8] and [7] for more details):

- Step 0. *Initialization.*

$$\text{With } u^0 \in V \text{ given} \tag{1.36}$$

  solve then

$$g^0 \in V, \ \ (g^0, v) = a(u^0, v) - L(v), \quad \forall v \in V. \tag{1.37}$$

  If $g^0 = 0$, or is *small*, take $u = u^0$; if not, set

$$w^0 = g^0. \tag{1.38}$$

  Then for $n \geq 0$, assuming that u^n, g^n, w^n are known, compute u^{n+1}, g^{n+1}, w^{n+1} as follows

- Step 1. *Descent.* Compute

$$\rho_n = \frac{\|g^n\|^2}{a(w^n, w^n)}, \tag{1.39}$$

and then

$$u^{n+1} = u^n - \rho_n w^n. \tag{1.40}$$

- Step 2. *Test of the convergence and construction of the new descent direction.* Solve

$$g^{n+1} \in V,$$

$$(g^{n+1}, v) = (g^n, v) - \rho_n a(w^n, v), \quad \forall v \in V; \tag{1.41}$$

if $g^{n+1} = 0$, or is *small*, take $u = u^{n+1}$; if not, compute

$$\gamma_n = \frac{\|g^{n+1}\|^2}{\|g^n\|^2}, \tag{1.42}$$

and define the new descent direction by

$$w^{n+1} = g^{n+1} + \gamma_n w^n. \tag{1.43}$$

Take $n = n + 1$ and go to (1.39).

If u is the solution of problem (1.35) we have (see [8])

$$\|u^n - u\| \leq C\|u^0 - u\| \left(\frac{\sqrt{\nu_a} - 1}{\sqrt{\nu_a} + 1}\right)^n, \tag{1.44}$$

where the *condition number* ν_a of $a(\cdot, \cdot)$ is defined by

$$\nu_a = \sup_{v \in V - \{0\}} \frac{a(v, v)}{\|v\|^2} \Big/ \inf_{v \in V - \{0\}} \frac{a(v, v)}{\|v\|^2}.$$

Back to the practical implementation of the algorithm, by g^{n+1} *small* we mean that g^{n+1} satisfy

$$\frac{\|g^{n+1}\|}{\|g^0\|} \leq \varepsilon,$$

where ε is a small positive number, that we refer as *tolerance*, depending upon the floating point arithmetic used by the computer (see [8] for more details).

1.4.2 Conjugate Gradient Solution of $\Lambda e = f$ in $1 - D$: Program elftos.m

The HUM reduces the calculation of the control of minimal L^2-norm for the continuous problem (1.3) to solving $\Lambda e = f$, with $f = \{-u^1, u^0\}$ given and $e \in E = H_0^1(a, b) \times L^2(a, b)$. In this subsection we adapt the general cg-algorithm described above to solve this linear problem. We first describe the algorithm at the continuous level and then we discuss the practical numerical implementation.

Continuous cg-algorithm

We take

$$V = E,$$

$$a(\cdot, \cdot) = \langle \Lambda \cdot, \cdot \rangle, \qquad L : \check{e} \to \langle \{u^1, -u^0\}, \check{e} \rangle.$$

The general cg-algorithm applied to the boundary control problem reads as follows:

- Step 0. *Initialization.* Choose a tolerance parameter $tolerance > 0$ and an initial guess for the solution

$$e_0^0 \in H_0^1(a,b) \text{ and } e_0^1 \in L^2(a,b). \tag{1.45}$$

As we have no idea about the possible solution, we take $e_0^0 = e_0^1 = 0$, for example.

The *tolerance* parameter provides a criterium to stop the program. Note that in general, we cannot expect a exact solution of the linear problem $\Lambda e = f$ due, in part, to the numerical round-off errors. Thus we must assume some "tolerance" to our algorithm and stop it when $\Lambda e - f$ is "sufficiently small". The *tolerance* parameter is, roughly, compared with $\Lambda e - f$, at each iteration, to decide if the algorithm stops.

Solve

$$\begin{cases} \phi_{0,tt} - \phi_{0,xx} = 0, & a < x < b, \quad 0 < t < T, \\ \phi_0 = 0, & 0 < t < T, \\ \phi_0(0) = e_0^0, \qquad \phi_{0,t}(0) = e_0^1, \end{cases} \tag{1.46}$$

and

$$\begin{cases} \psi_{0,tt} - \psi_{0,xx} = 0, & a < x < b, \quad 0 < t < T, \\ \psi_0(a) = 0, \quad \psi_0(b) = \phi_{0,x}(b,t), & 0 < t < T, \\ \psi_0(T) = \psi_{0,t}(T) = 0, & a < x < b. \end{cases} \tag{1.47}$$

Compute $g_0 = \{g_0^0, g_0^1\} \in E$,

$$-g_{0,xx}^0 = \psi_{0,t}(0) - u^1, \text{ in } (a,b), \quad g_0^0(a) = g_0^0(b) = 0. \tag{1.48}$$

$$g_0^1 = u^0 - \psi_0(0), \tag{1.49}$$

respectively. Set then

$$w_0 = g_0. \tag{1.50}$$

Now, for $n \geq 0$, assuming that e_n, g_n, w_n, ϕ_n, ψ_n are known, compute e_{n+1}, g_{n+1}, w_{n+1}, ϕ_{n+1}, ψ_{n+1} as follows:

- Step 1. *Descent.* Solve the systems

$$\begin{cases} \phi_{n,tt} - \phi_{n,xx} = 0, & a < x < b, \quad 0 < t < T, \\ \phi_n = 0, & 0 < t < T, \\ \phi_n(0) = w_n^0, \qquad \phi_{n,t}(0) = w_n^1, \end{cases} \tag{1.51}$$

and

$$\begin{cases} \psi_{n,tt} - \psi_{n,xx} = 0, & a < x < b, \quad 0 < t < T, \\ \psi_n(a) = 0, \quad \psi_n(b) = \phi_{n,x}(b,t), & 0 < t < T, \\ \psi_n(T) = \psi_{n,t}(T) = 0, & a < x < b, \end{cases} \tag{1.52}$$

$$-g_{n,xx}^0 = \psi_{n,t}(0), \text{ in } (a,b), \quad g_n^0(a) = g_n^0(b) = 0 \tag{1.53}$$

and set

$$g_n^1 = -\psi_n(0). \tag{1.54}$$

Compute now a numerical approximation of

$$\rho_n = \frac{\int_0^1 (|g_{n,x}^0|^2 + |g_n^1|^2) dx}{\int_0^1 (g_{n,x}^0 w_{n,x}^0 + g_n^1 w_n^1) dx}, \tag{1.55}$$

$$e_{n+1} = e_n - \rho_n w_n \tag{1.56}$$

$$\phi_{n+1} = \phi_n - \rho_n \phi_n \tag{1.57}$$

$$\psi_{n+1} = \psi_n - \rho_n \psi_n \tag{1.58}$$

$$g_{n+1} = g_n - \rho_n g_n. \tag{1.59}$$

The new residue is defined by

$$\text{residue} = \frac{\|g^{n+1}\|}{\|g^0\|}.$$

- Step 2. *Test of the convergence and construction of the new descent direction.* If $g_{n+1} = 0$, or is *small* (residue<*tolerance*), take $e = e_{n+1}$, $\phi = \phi_{n+1}$, $\psi = \psi_{n+1}$; if not, compute

$$\gamma_n = \frac{\int_0^1 (|g^0_{n+1,x}|^2 + |g^1_{n+1}|^2)dx}{\int_0^1 (|g^0_{n,x}|^2 + |g^1_n|^2)dx}, \tag{1.60}$$

and define the new descent direction by

$$w_{n+1} = g_{n+1} + \gamma_n w_n. \tag{1.61}$$

Set $n := n + 1$ and go to (1.55).

Numerical issues. Program elftos.m

The numerical implementation of the above algorithm is included in the subprogram *elftos.m*, which is part of the main program `wavecontrol`.

Program *elftos.m* is initialized with the following parameters: a, b (the left and right extremities of the domain), n (the number of internal nodes in the space discretization), r (the parameter to choose the mass matrix in the space discretization) T (the final time), $\mu = h/\Delta t$ (the courant number), *eps* (the tolerance), β, γ (the parameters of the Newmark method in the time discretization) and $(U^0, U^1) \in \mathbb{R}^{2n}$ (the value of the initial data to be controlled at the nodes).

The program follows the algorithm described above. To simplify, two internal functions are defined: forward.m, that solves the wave equations (1.46) and (1.51), and psiback.m that solves (1.47) and (1.52).

1.4.3 Conjugate Gradient Solution of $\Lambda e = f$ in $2 - d$

As in the 1-D case, the HUM reduces the calculation of the control of minimal L^2-norm for the continuous problem (1.11) to solving $\Lambda e = f$, with $f = \{-u^1, u^0\}$ given and $e \in E = H_0^1(\Omega) \times L^2(\Omega)$. In this subsection we adapt the general cg-algorithm described above to solve this linear problem. We first describe the algorithm at the continuous level and then we discuss the practical numerical implementation.

Continuous cg-algorithm

We take

$$V = E,$$

$$a(\cdot,\cdot) = \langle \Lambda \cdot, \cdot \rangle, \qquad L : \check{e} \to \langle \{u^1, -u^0\}, \check{e} \rangle.$$

We denote by

$$\Box = \frac{\partial^2}{\partial t^2} - \Delta, \quad \text{in} \quad \Omega \times (0, T)$$

the d'Alembert operator.

- Step 0. *Initialization.* Choose a positive value for the tolerance parameter, $tolerance > 0$, and the initial guess

$$e_0^0 \in H_0^1(\Omega) \text{ and } e_0^1 \in L^2(\Omega). \tag{1.62}$$

Solve

$$\begin{cases} \Box\phi_0 = 0, & \text{in} \quad \Omega \times (0,T), \\ \phi_0 = 0, & \partial\Omega \times (0,T), \\ \phi_0(0) = e_0^0, \qquad \dfrac{\partial\phi_0}{\partial t}(0) = e_0^1, & \text{in} \quad \Omega \end{cases} \tag{1.63}$$

and

$$\begin{cases} \Box\psi_0 = 0, & \text{in} \quad \Omega \times (0,T), \\ \psi_0 = \frac{\partial\phi_0}{\partial n}|_{\Gamma_1}, \quad \text{on } \Gamma_1 & 0 < t < T, \\ \psi_0 = 0, \quad \text{on } \partial\Omega\backslash\Gamma_1 & 0 < t < T, \\ \psi_0(T) = 0, \quad \frac{\partial\psi_0}{\partial t}(T) = 0, & \text{in} \quad \Omega. \end{cases} \tag{1.64}$$

Compute $g_0 = \{g_0^0, g_0^1\} \in E$,

$$-\Delta g_0^0 = \frac{\partial\psi_0}{\partial t}(0) - u^1, \text{ in } \Omega, \quad g_0^0 = 0, \quad \text{on } \partial\Omega. \tag{1.65}$$

$$g_0^1 = u^0 - \psi_0(0), \tag{1.66}$$

respectively. Set then

$$w_0 = g_0, \quad \text{in } \Omega. \tag{1.67}$$

Now, for $n \geq 0$, assuming that e_n, g_n, w_n, ϕ_n, ψ_n are known, compute e_{n+1}, g_{n+1}, w_{n+1}, ϕ_{n+1}, ψ_{n+1} as follows:

- Step 1. *Descent.* Solve the systems

$$\begin{cases} \Box\phi_n = 0, & \text{in} \quad \Omega \times (0,T), \\ \phi_0 = 0, & \text{on } \partial\Omega \times (0,T), \\ \phi_n(0) = w_n^0, \qquad \frac{\partial\phi_n}{\partial t}(0) = w_n^1, & \text{in} \quad \Omega \end{cases} \tag{1.68}$$

and

$$\begin{cases} \Box\psi_n = 0, & \text{in} \quad \Omega \times (0,T), \\ \psi_n = \frac{\partial\phi_n}{\partial n}|_{\Gamma_1}, \quad \text{on } \Gamma_1 & 0 < t < T, \\ \psi_n = 0, \quad \text{on } \partial\Omega\backslash\Gamma_1 & 0 < t < T, \\ \psi_n(T) = 0, \quad \frac{\partial\psi_n}{\partial t}(T) = 0, & \text{in} \quad \Omega. \end{cases} \tag{1.69}$$

$$-\Delta g_n^0 = \frac{\partial\psi_n}{\partial t}(0), \text{ in } \Omega, \quad g_n^0 = 0, \quad \text{on } \partial\Omega. \tag{1.70}$$

and set

$$g_n^1 = -\psi_n(0). \tag{1.71}$$

Compute now

$$\rho_n = \frac{\int_\Omega (|\nabla g_n^0|^2 + |g_n^1|^2)dx}{\int_\Omega (\nabla g_n^0 \nabla w_n^0 + g_n^1 w_n^1)dx}, \tag{1.72}$$

$$e_{n+1} = e_n - \rho_n w_n \tag{1.73}$$

$$\phi_{n+1} = \phi_n - \rho_n \phi_n \tag{1.74}$$

$$\psi_{n+1} = \psi_n - \rho_n \psi_n \tag{1.75}$$

$$g_{n+1} = g_n - \rho_n g_n. \tag{1.76}$$

The new residue is given by

$$\text{residue} = \frac{\|g_{n+1}\|_{H_0^1 \times L^2}}{\|g_0\|_{H_0^1 \times L^2}}.$$

- Step 2. *Test of the convergence and construction of the new descent direction.* If $g_{n+1} = 0$, or is *small* (residue< *tolerance*), take $e = e_{n+1}$, $\phi = \phi_{n+1}$, $\psi = \psi_{n+1}$; if not, compute

$$\gamma_n = \frac{\int_\Omega (|\nabla g^0_{n+1}|^2 + |g^1_{n+1}|^2)dx}{\int_\Omega (|\nabla g^0_n|^2 + |g^1_n|^2)dx}, \tag{1.77}$$

and define the new descent direction by

$$w_{n+1} = g_{n+1} + \gamma_n w_n. \tag{1.78}$$

Set $n := n + 1$ and go to (1.55).

Numerical issues. Program cont2d.m

The numerical implementation of the above algorithm is included in the subprogram cont2d.m, which is part of the main program `wavecontrol`.

Program cont2d.m is initialized with the following parameters: a, b (the left and right extremes of the square domain $(a, b) \times (a, b)$), n (the number of internal nodes in the space interval (a, b)), T (the final time), $\mu = \Delta t/h$ (the Courant number), *eps* (the tolerance) and $(U^0, U^1) \in \mathbb{R}^{2(n\times n)}$ (the value of the initial data to be controlled at the nodes).

The program follows the algorithm described above. To simplify, two internal functions are defined: forward.m, that solves the wave equations (1.63) and (1.68), and psiback.m that solves (1.64) and (1.69).

1.4.4 An implementation of the bi-Grid technique

For simplicity, we present the algorithm for the 1-D finite differences space semi-discretization. The 2-D case with a finite element implementation is analogous and we refer to [8] for a detailed description.

Let us introduce two grids of the interval (a, b). The fine one, by considering an odd number $N \in N$, $h = (b - a)/(N + 1)$ and $x_i = ih$, $i = 1, ..., N$; and the coarse one, with step $2h$, by taking $y_i = 2ih$, $i = 1, ..., (N - 1)/2$.

The main idea is to consider a space discretization scheme of the wave equations in the fine grid but taking the initial (or final) data in the coarse one. In this way, the high frequencies associated to the fine grid are eliminated.

Thus, in order to solve the wave equation in the fine grid we must define two operators. An interpolation operator I^h_{2h} which transform a vector data in the coarse grid $\{e^i_{2h}\}_{i=1,...,(N-1)/2}$ to a vector data in the fine one $\{e^i_h\}_{i=1,...,N}$; and a projection operator I^{2h}_h which transform a vector data in the fine grid $\{e^i_h\}_{i=1,...,N} \in R^N$ to a vector data in the coarse one $\{e^i_{2h}\}_{i=1,...,(N-1)/2} \in R^{(N-1)/2}$.

The simplest choice is:

$$\begin{aligned}
I^h_{2h}: &\quad R^{(N-1)/2} \to R^N \\
&\quad e_{2h} \to e_h, \quad \text{where } e^{2i}_h = e^i_{2h} \text{ and } e^{2i-1}_h = \tfrac{e^{i-1}_{2h} + e^i_{2h}}{2},\ i = 1, ..., (N-1)/2, \\
I^{2h}_h: &\quad R^N \to R^{(N-1)/2} \\
&\quad e_h \to e_{2h}, \quad \text{where } e^i_{2h} = e^{2i}_h,\ i = 1, ..., (N-1)/2.
\end{aligned}$$

Once defined these operators, the wave equation is solved as follows:

1. Interpolation of a given initial data in the coarse grid to obtain an initial data in the fine grid.

2. Solution of the wave equation in the fine grid.

3. Projection of the final data to obtain a result in the coarse grid.

We now describe the conjugate gradient algorithm with this bi-grid strategy.

Let us denote by M and K the mass and the stiffness matrices corresponding to the discretization on the fine grid. Let K_{2h} be the discretization of the Laplace operator, with homogeneous boundary Dirichlet conditions, in the coarse grid. We obtain then the following conjugate gradient algorithm:

- Step 0. *Initialization.* Choose a tolerance parameter $tolerance > 0$. Given

$$e^0_{0,2h} \in V_{0,2h} \text{ and } e^1_{0,2h} \in R^{(N-1)/2} \tag{1.79}$$

solve then, the discrete forward wave equation

$$\begin{cases} M\phi''_{0,h}(t) + K\phi_{0,h}(t) = 0, & 0 < t < T \\ \phi_{0,h}(0) = e^0_{0,h}, \quad \partial_t\phi_{0,h}(0) = e^1_{0,h}, \\ I^h_{2h}(e^0_{0,2h}) = e^0_{0,h}, \quad I^h_{2h}(e^1_{0,2h}) = e^1_{0,h} \end{cases} \tag{1.80}$$

and denote by $\phi_{0,h}$ the corresponding solution. The normal derivative at the extreme $x = b$ is approximated by $-\frac{1}{h}\phi^N_{0,h}(t)$ where $\phi^N_{0,h}(t)$ is the N-component of the vector $\phi_{0,h}(t) \in R^N$.

Solve the backward wave equation in the fine grid,

$$\begin{cases} M\psi''_{0,h}(t) + K\psi_{0,h}(t) = F_{0,h}, & 0 < t < T, \\ \psi_{0,h}(T) = \psi'_{0,h}(T) = 0. \end{cases} \tag{1.81}$$

The vector $F_{0,h} \in R^N$ has zero all its components but the last one, which contains the Dirichlet control at the extreme $x = b$, $-\frac{1}{h}\phi^N_{0,h}(t)$. Denote by $\psi_{0,h}$ the corresponding solution.

Restrict $\psi_{0,h}$ to the coarse space as follows:

$$\psi_{0,2h} = I^{2h}_h \psi_{0,h}.$$

Compute $g_0 = \{g^0_0, g^1_0\}$ solving the discrete problem,

$$K_{2h}(g^0_0) = (\psi'_{0,2h})(0) - I^{2h}_h u^1, \tag{1.82}$$

$$g^1_0 = I^{2h}_h u^0 - \psi_{0,2h}(0). \tag{1.83}$$

Set then

$$w_{0,2h} = g_0. \tag{1.84}$$

Now, for $n \geq 0$, assuming that e_n, g_n, $w_{n,2h}$, $\psi_{n,2h}$ are known, compute e_{n+1}, g_{n+1}, $w_{n+1,2h}$, $\psi_{n+1,2h}$ as follows:

- Step 1. *Descent.* Solve the system

$$\begin{cases} M\phi''_{n,h}(t) + K\phi_{n,h}(t) = 0, & \phi_{n,h}, \quad 0 < t < T \\ \phi_{n,h}(0) = w^0_n, \quad \partial_t\phi_{0,h}(0) = w^1_n, \\ I^h_{2h}(w^0_{n,2h}) = w^0_n, \quad I^h_{2h}(w^1_{n,2h}) = w^1_n \end{cases} \tag{1.85}$$

and denote by $\phi_{n,h}$ the corresponding solution. The normal derivative at the extreme $x = b$ is approximated by $-\frac{1}{h}\phi^N_{n,h}(t)$ where $\phi^N_{n,h}(t)$ is the N-component of the vector $\phi_{n,h}(t) \in R^N$.

Solve the backward wave equation

$$\begin{cases} M\psi''_{n,h}(t) + K\psi_{n,h}(t) = F_{n,h}, & 0 < t < T, \\ \psi_{n,h}(T) = \psi'_{n,h}(T) = 0. \end{cases} \tag{1.86}$$

The vector $F_{n,h} \in R^N$ has zero all its components but the last one, which contains the Dirichlet control at the extreme $x = b$, $-\frac{1}{h}\phi^N_{n,h}(t)$. Denote by $\psi_{0,h}$ the corresponding solution.

Restrict $\psi_{n,h}$ to the coarse space as follows:

$$\psi_{n,2h} = I_h^{2h}\psi_{n,h}.$$

Compute $g_n = \{g_n^0, g_n^1\}$ solving the discrete problem,

$$K_{2h}(g_n^0) = (\psi'_{n,2h})(0), \tag{1.87}$$

$$g_n^1 = -\psi_{n,2h}(0). \tag{1.88}$$

Compute now

$$\rho_n = \frac{((Kg_n^0, g_n^0) + |g_n^1|^2)}{(Kg_n^0, w_n^0) + (g_n^1, w_n^1)}, \tag{1.89}$$

$$e_{n+1} = e_n - \rho_n w_n \tag{1.90}$$

$$\psi_{n+1,2h} = \psi_{n,2h} - \rho_n \psi_{n,2h} \tag{1.91}$$

$$g_{n+1} = g_n - \rho_n g_n. \tag{1.92}$$

- Step 2. *Test of the convergence and construction of the new descent direction.* If $g_{n+1} = 0$, or is *small* (residue< *tolerance*), take $e = e_{n+1}$, $\psi = \psi_{n+1,2h}$; if not, compute

$$\gamma_n = \frac{((Kg_{n+1}^0, g_{n+1}^0) + |g_{n+1}^1|^2)}{((Kg_n^0, g_n^0) + |g_n^1|^2)}, \tag{1.93}$$

and set the new descent direction by

$$w_{n+1} = g_{n+1} + \gamma_n w_n. \tag{1.94}$$

Set $n := n + 1$ and go to (1.55).

END

Chapter 2

Program `wavecontrol`

2.1 Description

The program `wavecontrol` contains numerical codes for the control and stabilization of the wave equation in one and two space dimensions.

To start the program the user is requested to execute the command `wavecontrol` in the main Matlab window. The initial window will appear (see Figure 2.1) allowing you to choose among the four different problems that can be solved:

1. Control of the 1-D wave equation
2. Control of the 2-D wave equation
3. Stabilization of the 1-D wave equation
4. Stabilization of the 2-D wave equation.

The first two options (*Control of the* 1*-D wave equation* and *Control of the* 2*-D wave equation*) compute approximations of the boundary control of the wave equation by solving the discrete version of the linear systems (1.8) and (1.15) with a conjugate gradient algorithm.

Three different spatial semi-discretization schemes are available for solving the 1-D wave equation in the control problems:

- Finite differences
- Finite elements
- Mixed finite elements,

while for the spatial semi-discretization of the 2-D wave equation we have:

- Finite differences
- Mixed finite elements
- A bi-grid finite element scheme.

The last two options (*Stabilization of the* 1*-D wave equation* and *Stabilization of the* 2*-D wave equation*) compute the energy of the solution u of the discrete version of system (1.17). We consider finite-difference discretization schemes in space and time for (1.17) and (1.18), as we have seen in the above sections.

In the rest of this section we briefly describe the interactive window that appears when each one of the above options is selected.

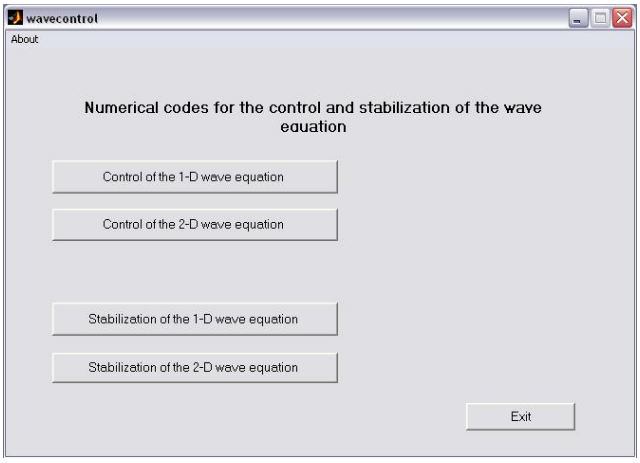

Figure 2.1: GUI of the program `wavecontrol`

2.1.1 Control of the $1-D$ wave equation

When selecting this option an interactive window appears (see figure 2.2) which contains three figures on the left hand side and a number of steps to follow, in the right hand side. In the two upper figures are represented the initial position and velocity to be controlled. The lower figure will contain the results and initially is empty.

In order to solve the control problem the user must follow the process described on the right hand side:

1. **Change parameters** This option allows you to select the values of the left and right extremes of the space interval a, b, the number of internal points n, the tolerance of the CG algorithm *tolerance*, the Courant number μ, the final time T, the parameters β, γ for the Newmark method (see Figure 2.3) and the mass matrix parameter r, $M = I + r\Delta$.

   Thus, we have two uniform meshes in space and time with step sizes

   $$h = \frac{b-a}{n+1} \quad \text{and} \quad \Delta t = \mu h.$$

   To obtain the three different discretization schemes (finite-differences, finite-elements or mixed finite elements) for (1.5)-(1.6), the user can:

   (a) change the parameters β, γ and r

   (b) leave the default parameters ($\beta = 0$, $\gamma = 1/2$, $r = 0$) and select directly the method (finite-difference, finite-elements or mixed finite elements) that appear in GUI and press the bottom **solution** (see Figure 2.2).

2. **Choose initial data** This option allows to choose one of four predefined examples or to edit new initial data. The chosen initial data will be represented in the upper figure windows.

3. **Choose method and press solution** This option allows to select the discretization method. There are three choices: finite differences, finite elements and mixed finite elements. See Figure 2.2.

   To obtain the solution the user must press the button Solution.

4. **Choose representation** This option allows to choose the magnitude to be plotted in the results figure (lower): control, solution, residue and animation.

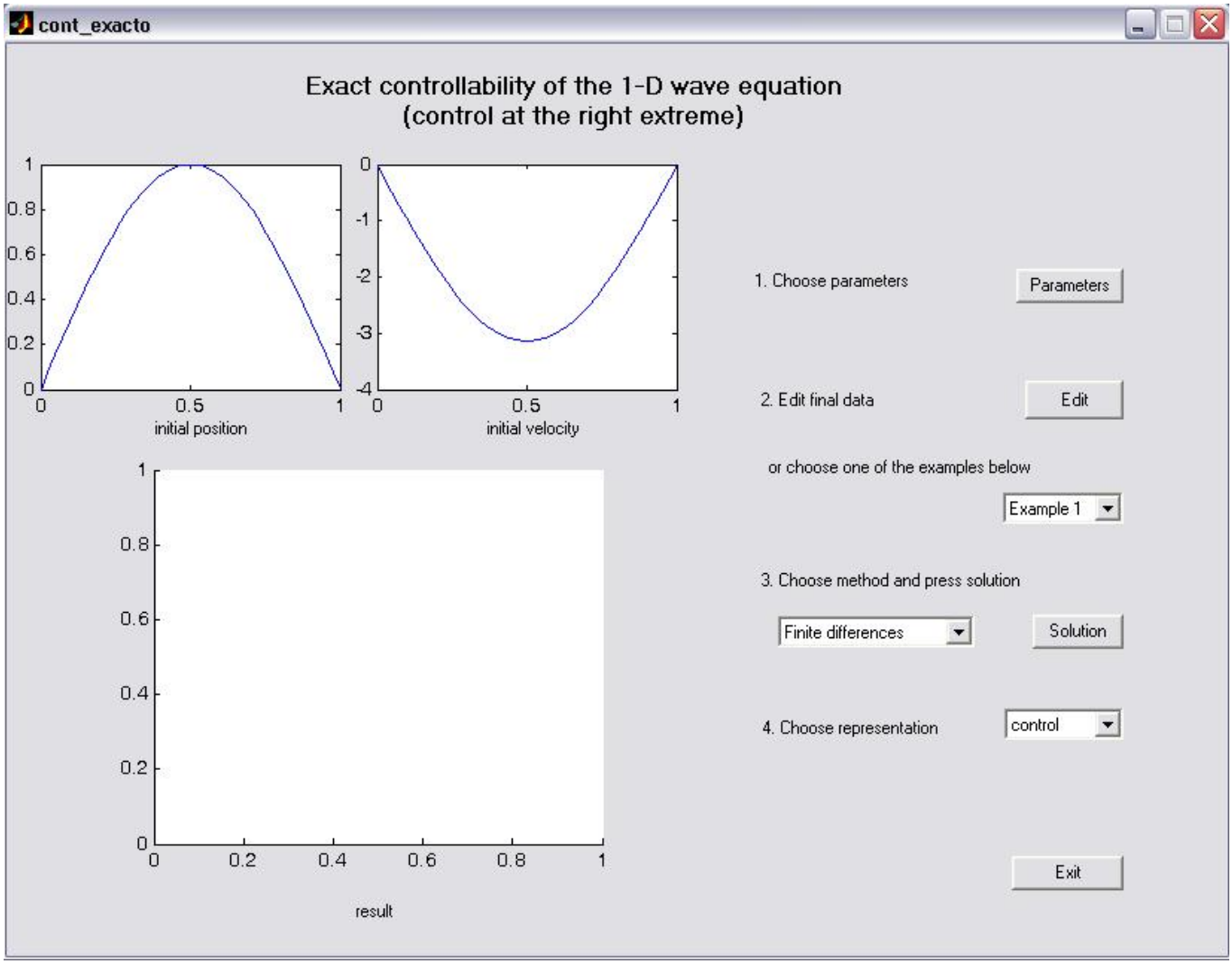

Figure 2.2: GUI for the program *Control of the* $1-D$ *wave equation*

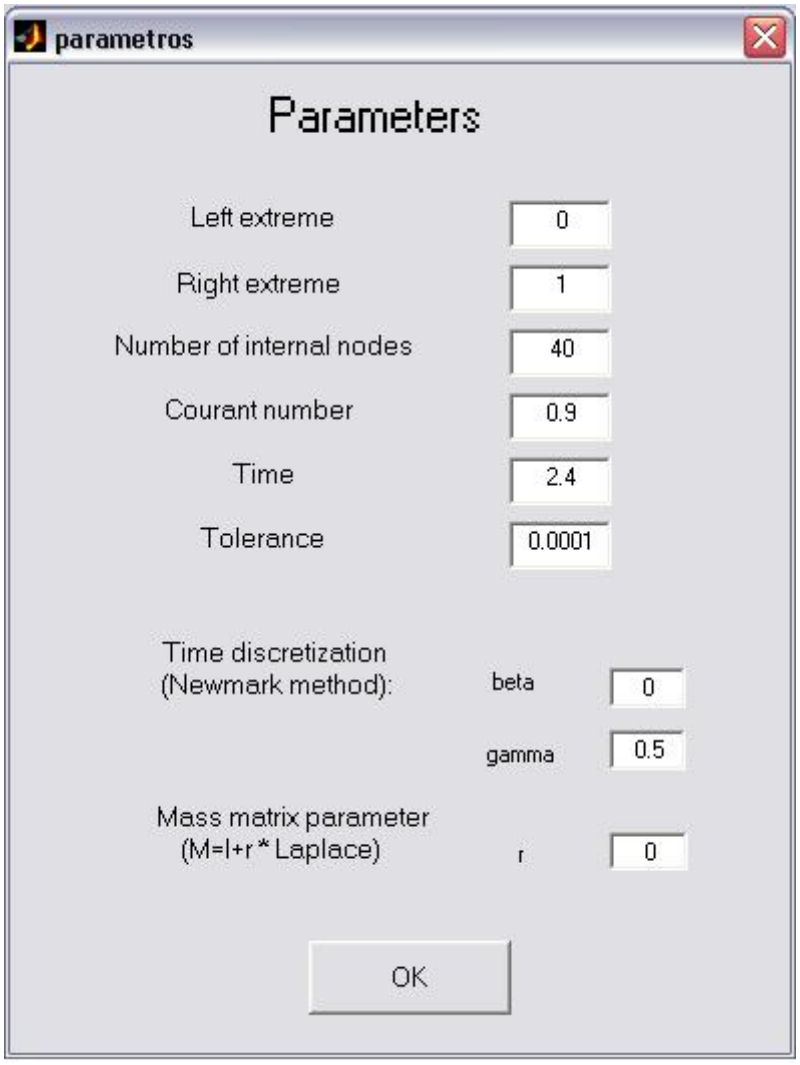

Figure 2.3: Choose *Parameters* window for *Control of the* $1-D$ *wave equation*

2.1.2 Control of the $2-d$ wave equation

When selecting this option an interactive window appears similar to the 1-D case (see figure 2.4). It contains three figures on the left hand side and a number of steps to follow, in the right hand side. In the two upper figures are represented the initial position and velocity to be controlled. The lower figure will contain the results and initially is empty.

In order to solve the control problem the user must follow the process described on the right hand side:

1. **Change parameters** This option allows you to select the values of the left and right extremes of the interval $[a, b]$; the domain being $[a, b] \times [a, b]$; the number of internal points of the space meshes n (uniform meshes in both space dimensions with the same steps); the tolerance of the CG algorithm *tolerance*; the Courant number μ and the final time T (see Figure 2.5).

2. **Choose initial data** To choose one of four predefined examples. A picture of the data to be controlled will be presented in the upper figures of the window.

3. **Choose method and press solution** Allows to select the discretization method. There are three choices: finite differences (FDS), mixed finite elements and bi-grid finite elements

(BI-GRID). See Figure 2.4.

To obtain the solution the user must press the button Solution.

4. **Choose representation** This option allows to choose the magnitude to be plotted in the results figure (lower one): control, residue and animation.

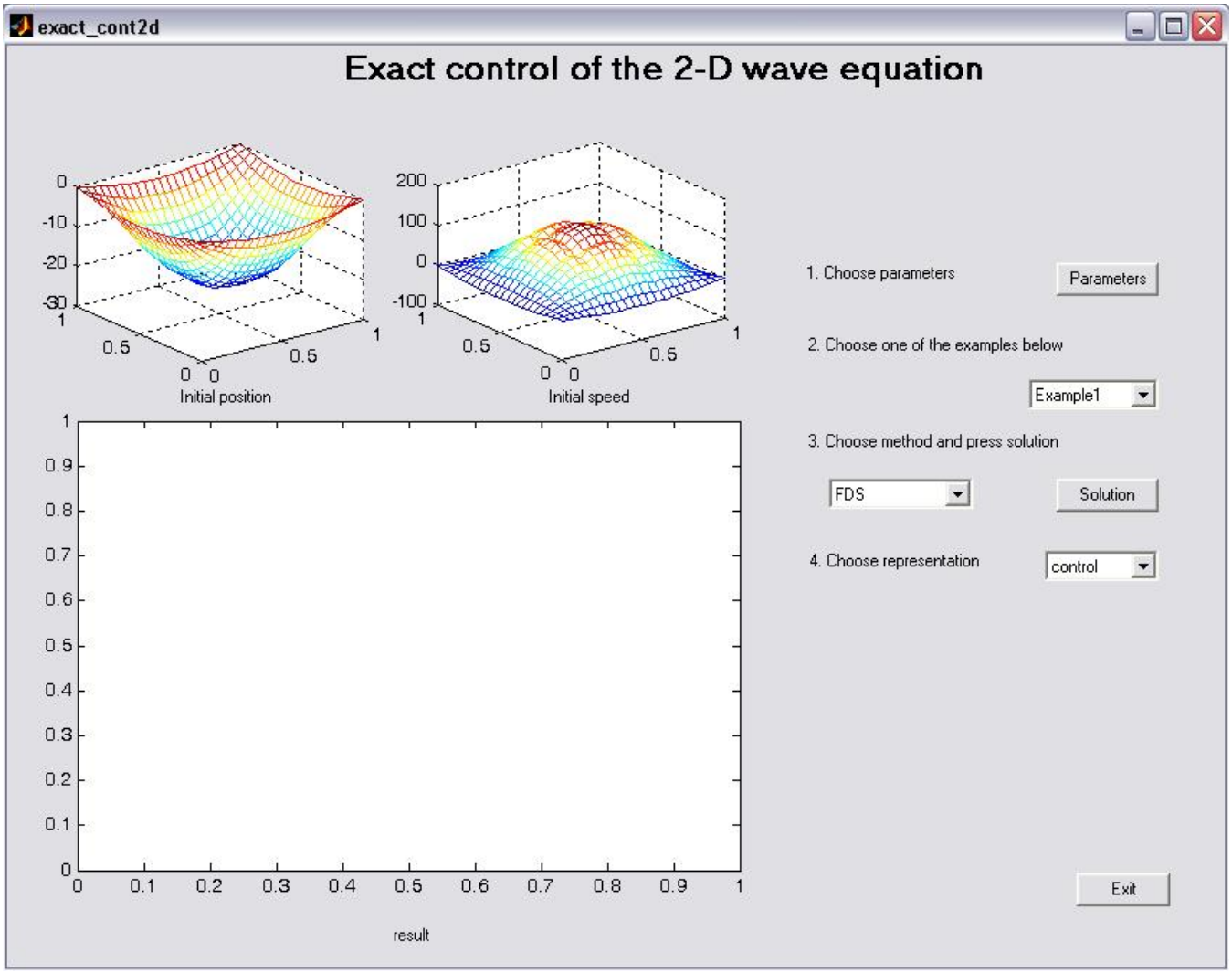

Figure 2.4: GUI for the program *Control of the* $2-d$ *wave equation*

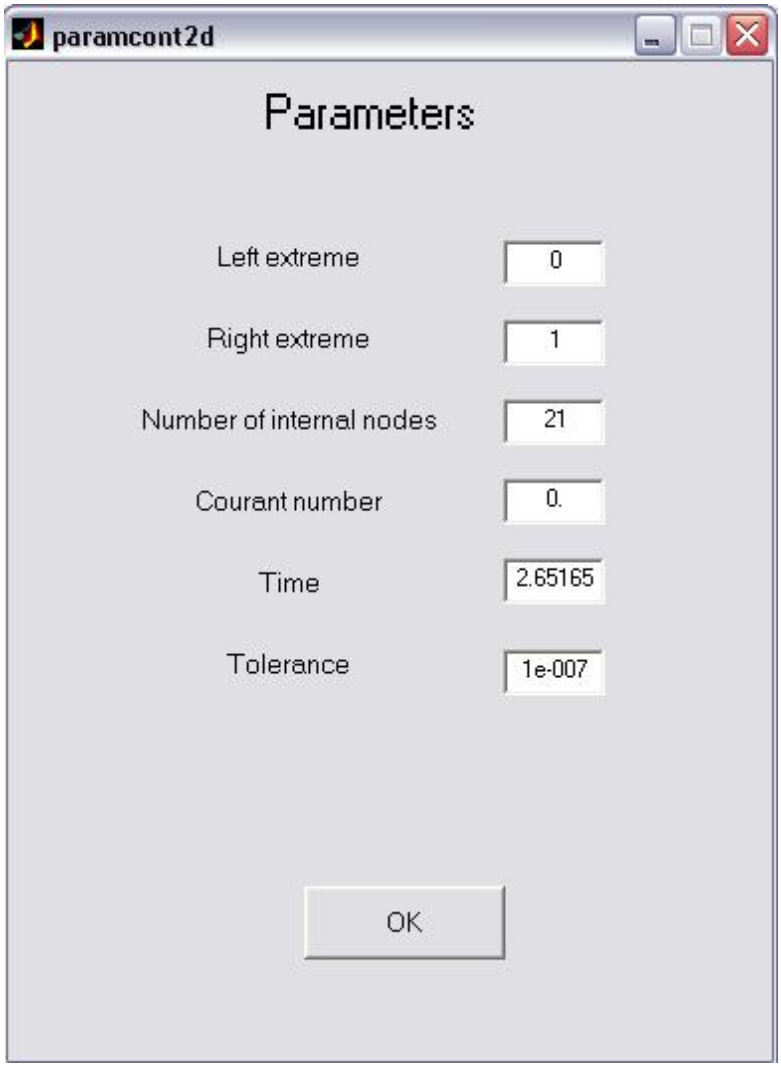

Figure 2.5: Choose *Parameters* window for *Control of the* $2-d$ *wave equation*

2.1.3 Stabilization of the $1-D$ wave equation

When selecting this option a new interactive window appears. It contains three figures on the left hand side and a number of steps to follow, in the right hand side. In the two upper figures are represented the initial position and velocity to be stabilized. The lower figure will contain the results and initially is empty.

The user must follow the process described on the right hand side:

1. **Change parameters** This option allows the user to select the values of the left and right extremes of the space interval a, b, the number of internal points in the mesh n, the Courant number μ, the final time T, the damping c, the viscosity parameters: α and β*–damping left and right extreme* and ν*– viscosity* (see Figure 2.7).

2. **Choose initial data** To choose one of four predefined examples or to edit new initial data. The initial data will be represented in the upper figures.

3. **Choose method and press solution** Allows to select the discretization method. There are three choices: finite differences, finite elements and mixed finite elements. See Figure 2.6.

   The user must then press button Solution.

4. **Choose representation** Allows to choose the magnitude to be plotted in the results figure (lower one): energy and animation.

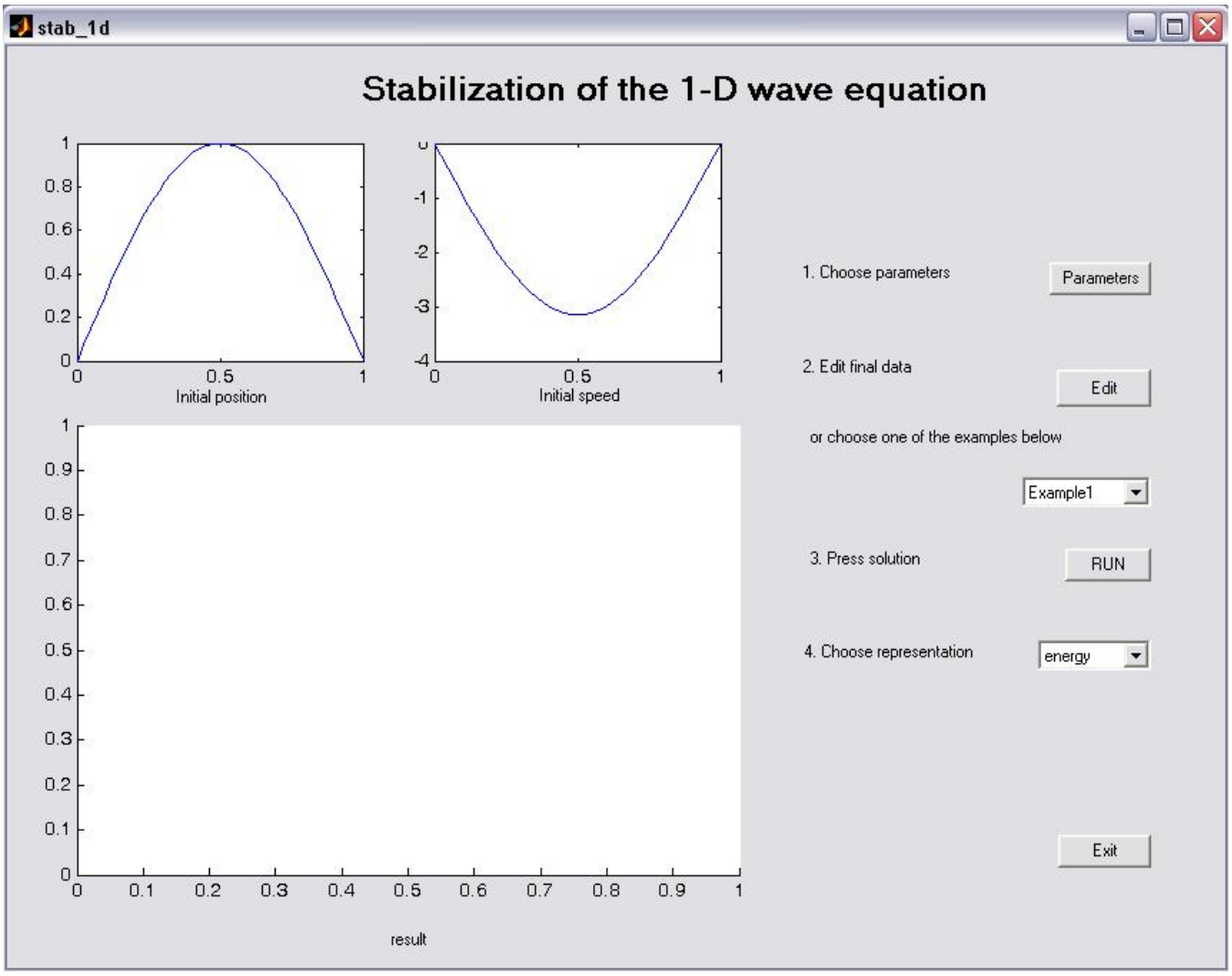

Figure 2.6: GUI for the program *Stabilization of the* $1-D$ *wave equation*

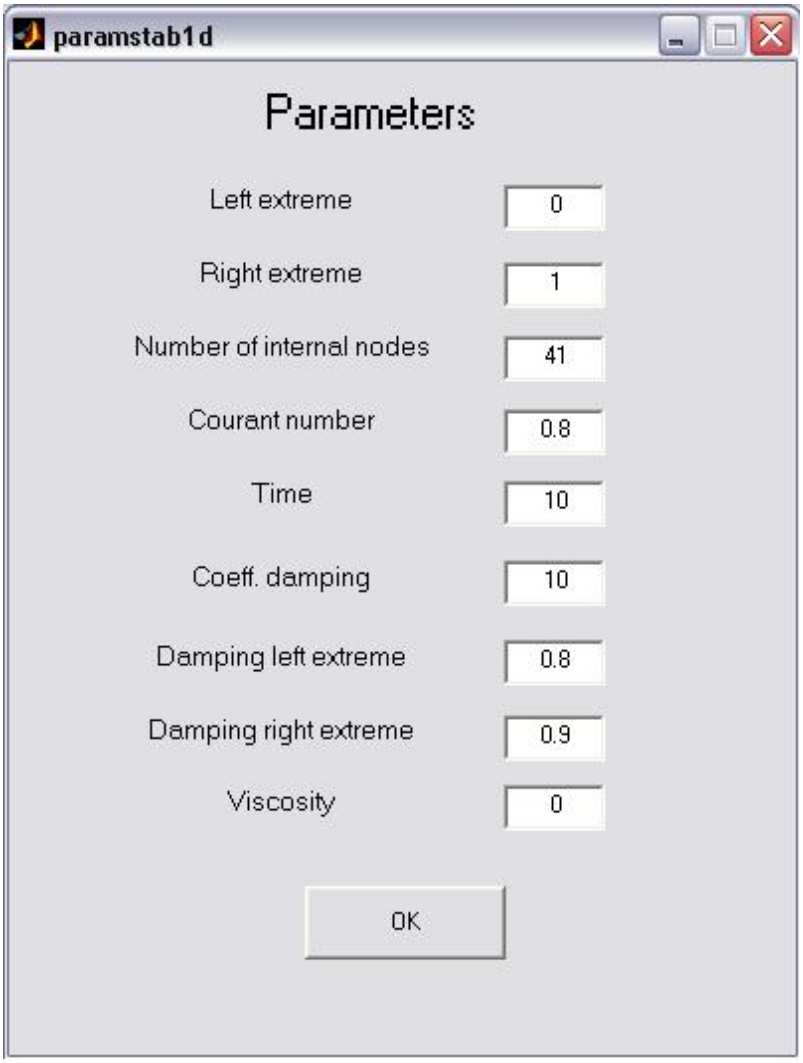

Figure 2.7: Choose *Parameters* window for *Stabilization of the* $1-D$ *wave equation*

2.1.4 Stabilization of the $2-d$ wave equation

When selecting this option a corresponding interactive window appears. As in the previous cases, it contains three figures on the left hand side and a number of steps to follow, in the right hand side. In the two upper figures are represented the initial position and velocity to be stabilized. The lower figure will contain the results and initially is empty.

The user must follow the process described on the right hand side:

1. **Change parameters** This option allows the user to select the values of the left and right extremes of the space interval $[a, b]$, the domain being $[a, b] \times [a, b]$; the number of internal points of the space meshes n (uniform meshes in both space dimensions with the same steps); the Courant number μ; the final time T; the damping c and the viscosity parameters: α and *β–damping left and right extreme*, and *ν– viscosity* (see Figure 2.9).

2. **Choose initial data** To choose one of four predefined examples that will be represented in the upper figures.

3. **Press solution** You should then press button Solution. See Figure 2.8.

4. **Choose representation** This option allows to choose the magnitude to be plotted in the results window (lower one): energy and animation and damping band (the sub-domain where the damping acts).

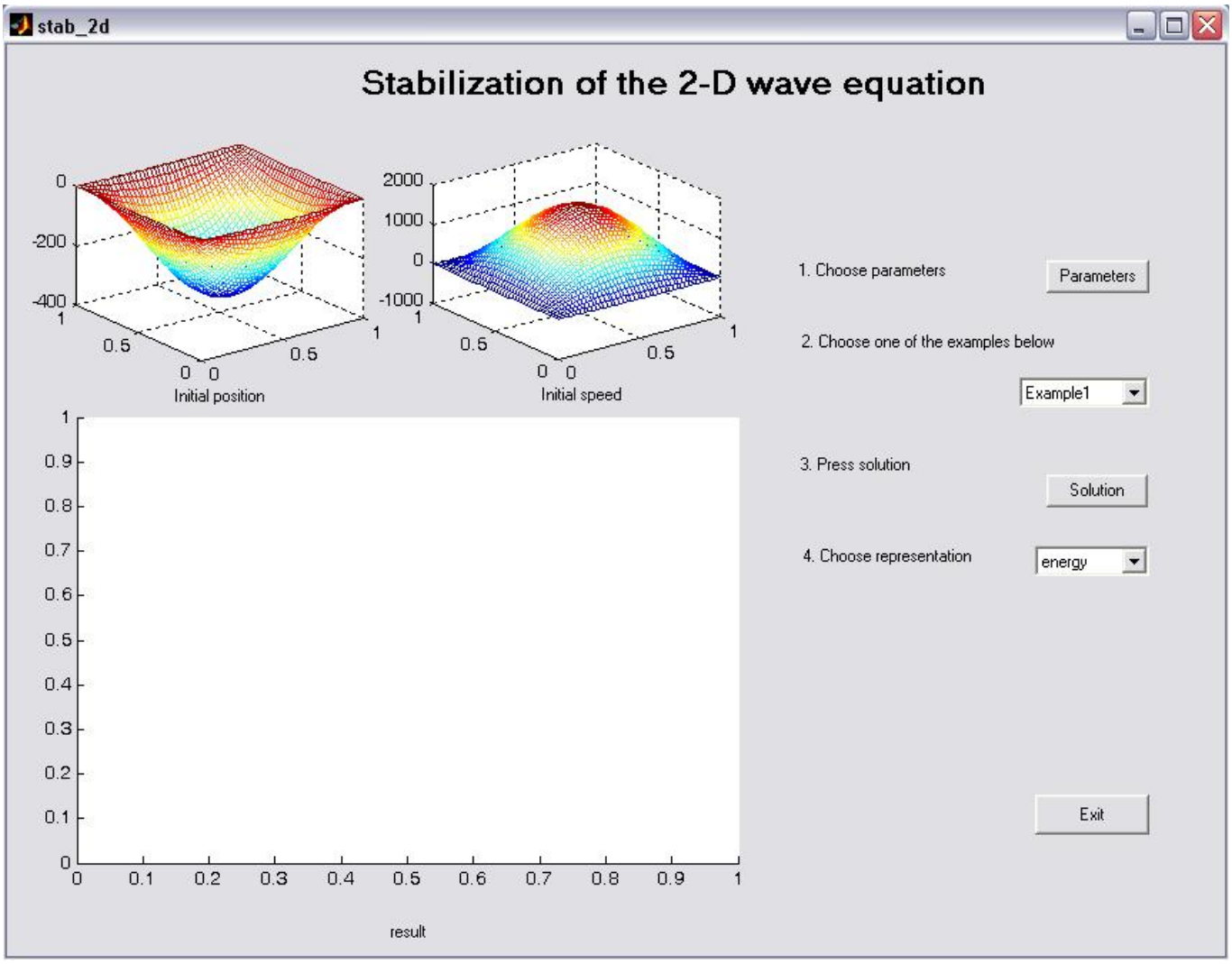

Figure 2.8: GUI for the *Stabilization of the* $2-d$ *wave equation*

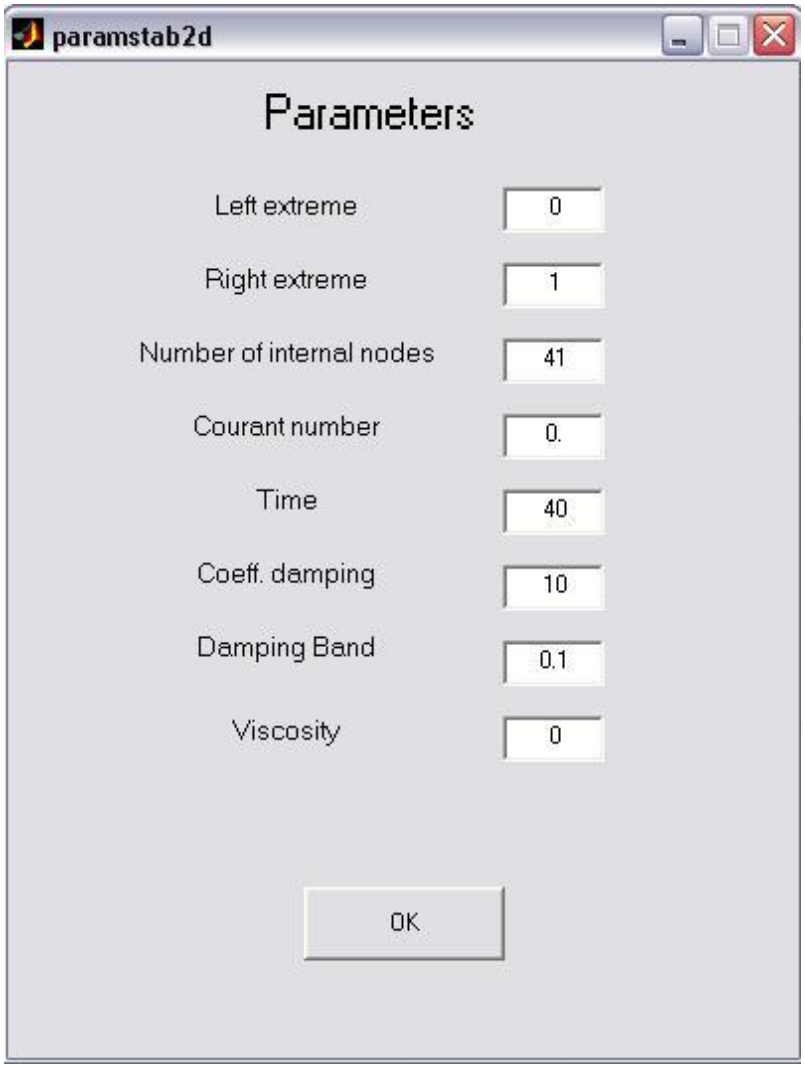

Figure 2.9: Choose *Parameters* window for *Stabilization of the* $2-d$ *wave equation*

Chapter 3

Examples

In Chapter one we pointed out the main difficulties arising when we try to find numerical approximations of the exact boundary control for the wave equation, or when we try to obtain the decay rate for the wave equation with internal damping. We also described some non-classical methods to discretize the wave equation (as the mixed finite elements for the control problem) and cures (as the bi-grid approach to the control problem or the numerical viscosity for the stabilization problem) that are well adapted to these type of problems.

In this chapter we comment some selected examples that somehow illustrate both the ill-conditioning of the control algorithm when using classical methods to approximate de wave equation and the efficiency of the proposed methods and cures.

3.1 Control of the 1-D wave equation

We focus on the results that one obtains for the particular initial data given in Example 2 ($u0 = x$ if $x \in [0, 0.5]$, $u0 = 0$ if $x > 0.5$ and $u1 = 0$). Note that this initial data is discontinuous at $x = 0.5$. This means in particular that the energy associated to the high frequency modes is large.

When considering central difference discretization in space and time with the Courant number $\mu = 1$, the control algorithm converges. In this case, it is well-known that the solution of the fully-discrete approximative system for the wave equation provides the exact solution of the continuous wave equation at the nodes (see [10], for example). Moreover, in [19] it is proved the convergence of the numerical solution of the discrete control problem to the exact HUM control of the continuous problem (see Figure 3.1).

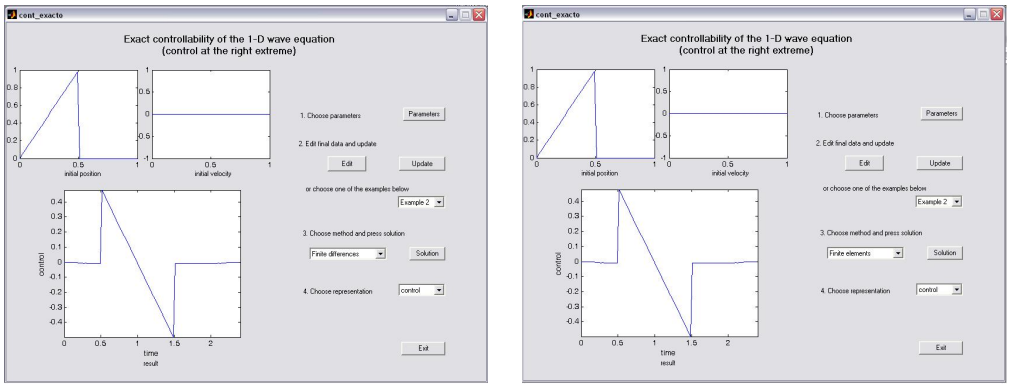

Figure 3.1: *Control* using *finite differences* (left) and *finite elements* (right) with $\mu = 1$– *CONVERGENCE of the cg-algorithm and CONVERGENCE of the control*

When $\mu < 1$, the dispersion diagrams predict that the controls will diverge, as $h \to 0$, except

if we use some filtering technique. In fact, the cg-algorithm does not converge in this case.

We now consider the mixed finite elements method in space with the implicit scheme in time. When $\mu = 0.9$, the *cg-* algorithm converges, the controls present oscillations but they are still bounded as h becomes small.

For smaller values of μ, for example $\mu = 0.1$, the numerical control is similar to the one computed with central differences with $\mu = 1$ (see 3.2).

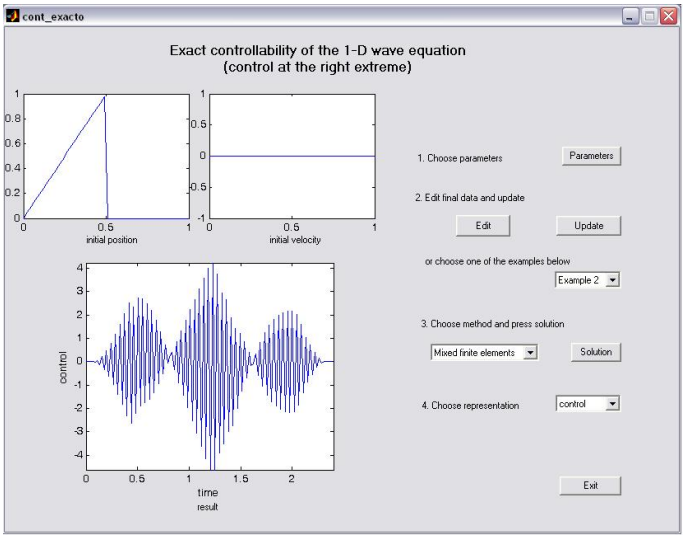

Figure 3.2: *Control* using mixed finite elements with $\mu = 0.9$–CONVERGENCE *of the cg-algorithm* and *bounded oscillating control*

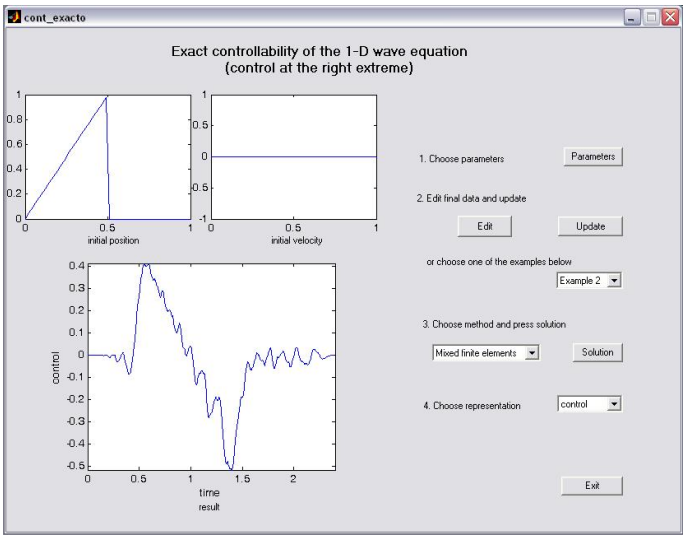

Figure 3.3: *Control* using mixed finite elements with $l = 0.1$–*CONVERGENCE of the cg-algorithm and of the control*

3.2 Exact control of the 2-D wave equation

We focus on the results obtained for the initial data given by Example 2, for different values of h (mesh-size), $h = 1/8$, $h = 1/16$, $h = 1/32$, $h = 1/64$ with the Courant number $\mu = 1/\sqrt{2}$ (corresponding to the upper limit in the stability condition).

It is interesting to see the deterioration of the numerical results as h and Δt tend to zero. Indeed, as was observed in [1] and [6], for $h \geq 1/32$ the numerical results are quite good but, for $h < 1/32$ the *cg*–algorithm diverges. When the initial data have an important high frequency contribution, the controls diverge when $h \to 0$ for the finite-difference scheme, except if we use some filtering technique or the bi-grid method. It is clear that the source of divergence in the limit process as $h \to 0$ in the exact controllability problem is the requirement of driving the high frequency components of the numerical solution exactly to zero.

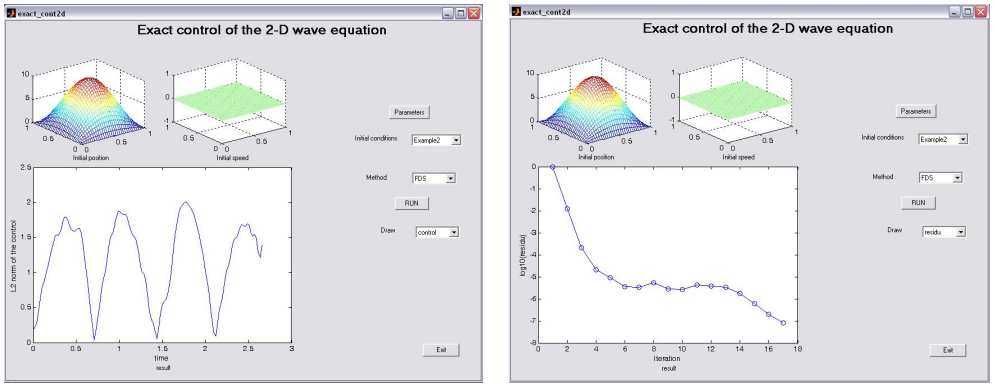

Figure 3.4: *L^2-norm of the control* (left) and *log(residue)* using finite differences $h = 1/32$, $\mu = 1/\sqrt{2}$

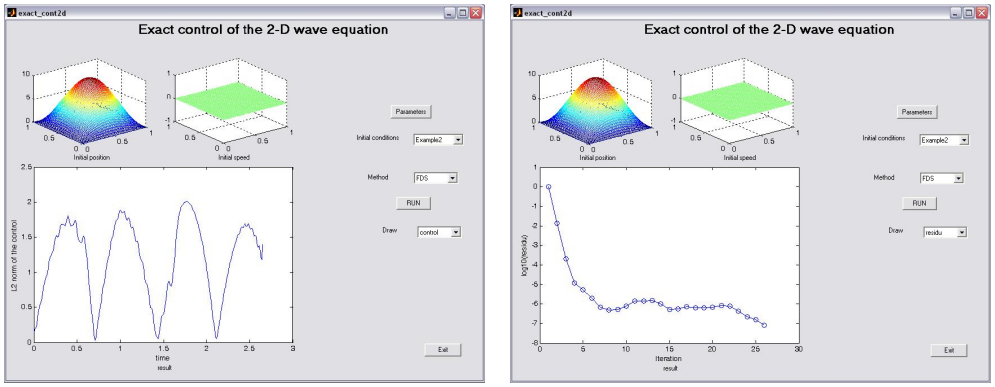

Figure 3.5: *L^2-norm of the control* (left) and *log(residue)* using finite differences $h = 1/64$, $\mu = 1/\sqrt{2}$

We consider now the same Example 2 and we present the numerical experiments applying the bi-grid algorithm described below. Comparing these results to those obtained using the finite-difference method, the following facts appear quite clearly:

1. The bi-grid algorithm method described in Section 1.5.4 is a very effective cure to the ill-posedness of the approximation of problem $\Lambda e = f$ (non-convergence of the conjugate gradient algorithm, large oscillations of the numerical control and non-convergence of this control to the real continuous control of the wave equation).

2. The number of conjugate gradient iterations to achieve the convergence is essentially independent of h. This does not happen in the finite-difference method (see [1] and [6] for more details).

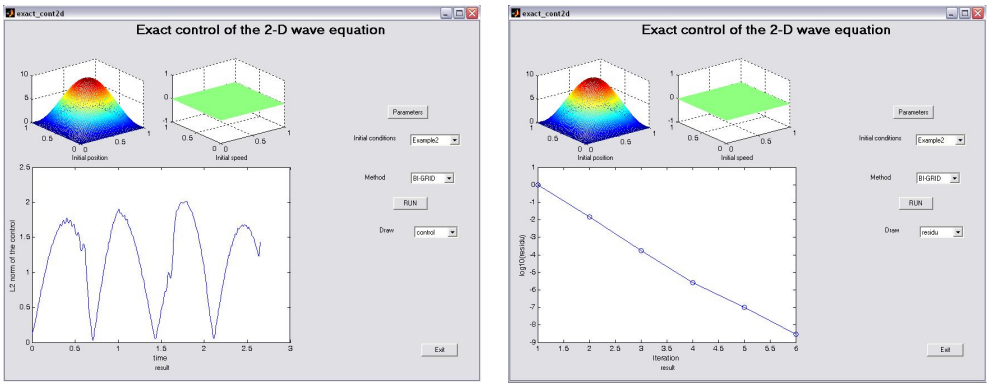

Figure 3.6: *L^2-norm of the control* (right) and *log(residue)* (left) using BI-GRID $h = 1/128$

3.3 Stabilization of the 1-D wave equation

Here we show the energy decay in the time interval $(0, T)$, with $T = 40$, for the initial data in Example 2 ($u0 = x$ if $x \in [0, 0.5]$, $u0 = 0$ if $x > 0.5$ and $u1 = 0$) and different values of the number of internal points n. We do it with and without numerical viscosity term (see 3.8). In these examples we have chosen the damping coefficient $c = 10$, the damping subinterval being $(\alpha, \beta) = (0.8, 0.9)$.

The straight line represents the graph of the polynomial P of degree T that fits the data, $P(t_m) = E(t_m)$, in a least-squares sense (see Matlab Help on command `polyfit` for details).

We can observe that the exponential energy decay degenerates as n increases (h decreases) when no viscosity is added. On the contrary, when the viscosity term is added to the equation, the exponential decay seems to be uniform in h in accordance to the theoretical results in [23].

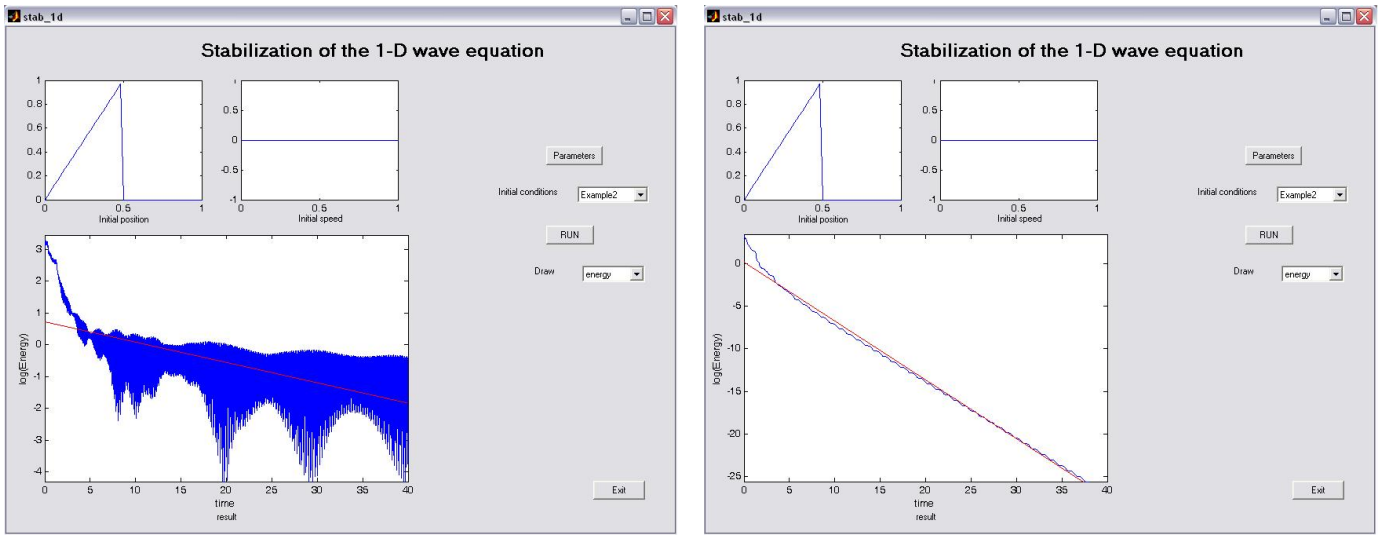

Figure 3.7: *log(Energy)* of the solution with $n = 61$ without (left) and with (right) viscosity in time $T = 40$

3.4 Stabilization of the 2-D wave equation

We show the energy decay in the time interval $(0, T)$, with $T = 60$, obtained for the initial data in Example 2 (the same as those used in the $2 - D$ control problem) and different values of the number of internal points n. This is done with and without viscosity term (see Figure 3.8). In these examples we have chosen the damping coefficient $c = 10$ and the width of the damping band 0.1 (see the sub-domain, where the damping acts in Figure 3.9 for $n = 61$).

As in the $1 - D$ case, we observe that the exponential energy decay degenerates as n increases when no viscosity is added. On the contrary, when the viscosity term is added to the equation, the exponential decay seems to be uniform in h.

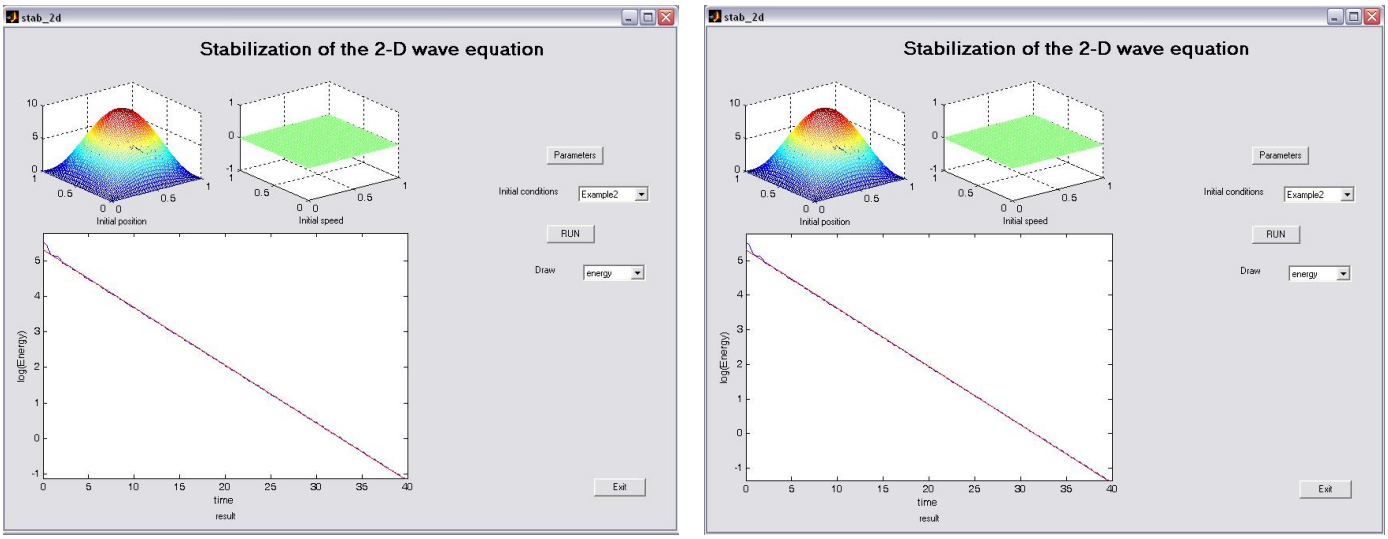

Figure 3.8: *log(Energy)*of the solution with $n = 61$ without (left) and with (right) viscosity in time $T = 40$

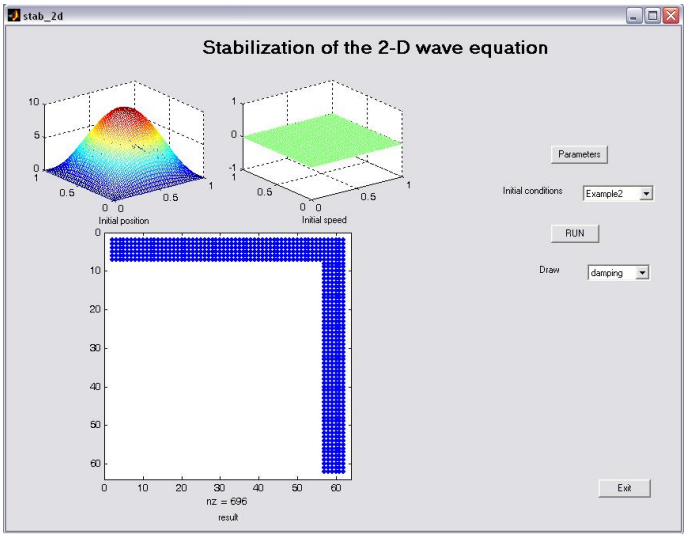

Figure 3.9: Stabilization of the 2-D wave equation in action– *damping sub-domain* in time $T = 40$

Bibliography

[1] M. Asch, G. Lebeau, *Geometrical aspects of exact boundary controllability for the wave equation-A numerical study*, ESAIM: Control, Optimization and Calculus of Variations, **3** (1998), 163-212.

[2] Banks H. T., Ito K. and Wang C., *Exponentially stable approximations of weakly damped wave equations.* Estimation and control of distributed parameter systems (Vorau, 1990), 1–33, Internat. Ser. Numer. Math., **100**, Birkhäuser, Basel, 1991.

[3] B. Bardos, G. Lebeau, J. Rauch, *Sharp sufficient conditions for the observation, control and stabilization from the boundary*, SIAM J. Control and Opt. **30**, 1024-1065, 1992.

[4] C. Castro and S. Micu, *Boundary controllability of a linear semi-discrete 1-D wave equation derived from a mixed finite elements method*, Numerische Mathematik, to appear.

[5] C. Castro, S. Micu and A. Münch, *Numerical approximation of the boundary control of the 2-d wave equation with mixed finite elements*, preprint 2005.

[6] R. Glowinski, *Ensuring well-posedness by analogy; Stokes problem and boundary control of the wave equation*, J. Compt. Phys., **103**(2), 189-221, 1992.

[7] R. Glowinski and J.-L. Lions, *Exact and approximate controllability for distributed parameter systems*, Acta Numerica, 159-333, 1996.

[8] R. Glowinski, C. H. Li, J.-L. Lions, *A numerical approach to the exact boundary controllability of the wave equation (I). Dirichlet controls: Description of the numerical methods*, Japan J. Math. Pures Appl., **68** (7), 1-76, 1990.

[9] Glowinski R., Kinton W. and Wheeler M. F., *A mixed finite element formulation for the boundary controllability of the wave equation*, Int. J. Numer. Methods Eng. **27(3)**, (1989), 623-636.

[10] T. Hughes, *The finite element method*, Prentice Hall.

[11] J.A. Infante and E. Zuazua, *Boundary observability for the space discretization of the one-dimensional wave equation*, M^2AN **33** (2) (1999), 407-438.

[12] Kappel F. and Ito K., *The Trotter-Kato theorem and approximations of PDE's*, Math. of Comput., **67** (1998), 21-44.

[13] J. L. Lions, *Contrôlabilité exacte, stabilisation et perturbations du systemes distribués. Tome 1 Contrôlabilité exacte*, Masson, RMA8, 1988.

[14] S. Micu, Uniform boundary controllability of a semi-discrete 1-D wave equation, Numerische Mathematik **91** (4) (2002), 723-768.

[15] A. Münch, *Family of implicit schemes uniformly controllable for the 1-D wave equation*, C. R. Acad. Sci. Paris, **339** (2004), 733-738.

[16] A. Münch, *A uniformly controllable and implicit scheme for the 1-D wave equation*, Mathematical Modelling and Numerical Analysis, **39** (2) (2005), 377-418.

[17] A. Münch and A. Pazoto, *Uniformly stabilization of a numerical approximation of a locally damped wave equation*, Preprint 2004.

[18] N. M. Newmark, *A Method of Computation for Structural Dynamics*, Journal of the Engineering Mechanics Division, ASCE, 67-94, 1959.

[19] M. Negreanu and E. Zuazua, *Uniform boundary controllability of a discrete* $1-D$ *wave equation*, Systems and Control Letters **48** (3-4) (2003), 261-279.

[20] M. Negreanu and E. Zuazua, *Discrete Ingham inequalities and applications*, C. R. Acad. Sci. Paris, Série I **338** (4) (2004), 281-286.

[21] M. Negreanu and E. Zuazua, *Convergence of a multigrid method for the controllability of a 1-D wave equation*, C. R. Acad. Sci. Paris, Série I **338** (5) (2004), 413-418.

[22] Raviart P. A. and Thomas J.-M., INTRODUCTION À L'ANALYSE NUMÉRIQUE DES ÉQUATIONS AUX DÉRIVÉES PARTIELLES, Masson, Paris, 1983.

[R] D. L. Russell, *Controllability and stabilizability theory for linear partial differential equations. Recent progress and open questions. SIAM Rev.*, **20**, (1978), 639-739.

[23] L. R. Tcheugoué Tébou, E. Zuazua, *Uniform exponential long time decay for the space semi-discretization of a locally damped wave equation via an artificial numerical viscosity*, Numerische Mathematik **95** (3)(2003) 563–598.

[24] E. Zuazua, *Propagation, Observation, Control of Waves Approximated by Finite Difference Methods*, SIAM Review, **47** (2) (2005), 197–243.

Chapter 4

Appendix: Dispersion Diagrams

In this section we present the dispersion relations for some of the numerical methods described to approximate the wave equation. The analysis of these dispersion relations allows to determine the velocity of propagation for the discrete dynamics associated to each numerical method and provides a necessary condition to have a uniform controllable numerical scheme. More precisely, a uniform controllable numerical scheme, with respect to the discretization parameters, must have a *uniformly bounded from below velocity of propagation of all waves*. Otherwise, the discrete controls in fixed time $T > 0$ could diverge, as the discretization parameters go to zero.

First of all, we introduce some classical concepts and notations. To fix ideas we focus on the $2-d$ case.

We consider the wave equation

$$\phi_{tt} - \Delta\phi = 0.$$

This equation admits plane wave solutions of the form

$$\phi(x,t) = e^{i(\xi\cdot x - \omega t)}, \quad \xi \in \mathbb{R}^2,\ \omega \in \mathbb{C}. \tag{4.1}$$

The constant vector $\xi = (\xi_1, \xi_2)$ is the *wave number* or *vibration mode* and ω is the *frequency*. The relationship

$$\omega = \omega(\xi), \quad \omega = \pm\xi \tag{4.2}$$

is known as the *dispersion relation* for the equation.

Any individual *'monochromatic wave'* (involving only one Fourier component) of (4.1) moves at the *phase velocity*

$$c(\xi,\omega) = \frac{\omega(\xi)}{|\xi|}. \tag{4.3}$$

The energy of wave packets propagates at the so-called *group velocity*

$$C(\xi,\omega) = \nabla_\xi \omega(\xi). \tag{4.4}$$

For any semi-discrete approximation of the wave equation we can also define the plane wave solutions. We consider a uniform discrete mesh $\{(x_i, x_j)\}$ of $\mathbb{R}^2$ with size step h in both variables. In this case, the semi-discrete equation admits solutions of type

$$\phi_{i,j}(t) = e^{i(\xi\cdot(x_i,x_j) - \omega t)}.$$

The relation $\omega = \omega(\xi)$ for which this plane waves are solutions of the semi-discrete model is known as the dispersion relation of the semi-discrete model.

In general, the dispersion relation for a partial differential equation is a polynomial relation between ξ and ω, while a discrete model has a $2\pi/h$–periodic trigonometric relation. Thus, it is natural to take $\xi \in [-\pi/h, \pi/h]^2$ as a fundamental domain.

The same analysis can be developed for fully discrete schemes. Considering numerical plane waves

$$\phi^n_{i,j} = e^{i(\xi\cdot(ih,jh) - \omega n\Delta t)},$$

one obtains the dispersion relation $\omega = \omega(\xi)$ of the fully-discrete model. Note that it is $2\pi/h$-periodic in ξ and $2\pi/\Delta t$-periodic in ω.

As we have said, in order to have a uniform controllable scheme we need a uniform bound from below of the velocity of propagation of all waves. This means that, if $\omega(\xi)$ is the dispersion relation of the numerical scheme, we must have

$$\|\nabla_\xi \omega(\xi)\| \geq C$$

with C independent of ξ and the discretization parameters involved.

Note that for the continuous wave equation $\omega(\xi) = \xi$ and $\|\nabla_\xi \omega(\xi)\| = 1$.

We now study separately the 1-D and 2-D numerical schemes.

4.0.1 1-D numerical schemes for the wave equation

We divide this section in two more subsections where we study the semi-discrete schemes and the fully-discrete ones respectively.

Semi-discrete schemes

We consider two particular space semi-discretization schemes: finite difference (FD) and mixed finite element (MFE). To distinguish the continuous and semi-discrete frequencies we denote:

- ω the frequency of the continuous problem
- ω_d the frequency of the FD semi-discrete problem
- ω_e the frequency of the MFE semi-discrete problem.

For the continuous wave equation, we have $\omega(\xi) = \xi$ and therefore $c(\xi) = C(\xi) = 1$. This corresponds to the fact that, for the continuous wave equation, the velocity of propagation of all waves is one.

For the FD semi-discrete scheme, the dispersion relation is

$$\omega_d(\xi) = \pm \frac{2}{h} \sin \frac{\xi h}{2}, \quad \xi \in \left[-\frac{\pi}{h}, \frac{\pi}{h} \right]. \tag{4.5}$$

The corresponding group velocity is

$$C(\xi, \omega_d) = \frac{d\omega_d(\xi)}{d\xi} = \cos \frac{\xi h}{2}, \tag{4.6}$$

tends to zero as $\xi \to \pm\pi/h$. In other words, high frequency waves propagate slower and slower as $h \to 0$.

For the MFE semi-discrete scheme, the dispersion relation is

$$\omega_e(\xi) = \frac{2}{h} \tan \frac{\xi h}{2}, \quad \xi \in \left[-\frac{\pi}{h}, \frac{\pi}{h} \right]. \tag{4.7}$$

The corresponding group velocity is

$$C(\xi, \omega_e) = \frac{d\omega_e(\xi)}{d\xi} = 1 + \tan^2 \frac{\xi h}{2}, \quad \xi \in \left[-\frac{\pi}{h}, \frac{\pi}{h} \right]. \tag{4.8}$$

Note that $C(\xi, \omega_e) \geq 1$ and tends to infinity when $\xi \approx \pm\pi/h$. Thus, for this semi-discrete system the velocity of propagation of all semi-discrete waves is uniformly bounded from below.

In Figure 4.1 we show the dispersion of the high vibration modes of the numerical semi-discrete schemes with finite difference and mixed finite element. We have taken $\xi \in [0, 40]$.

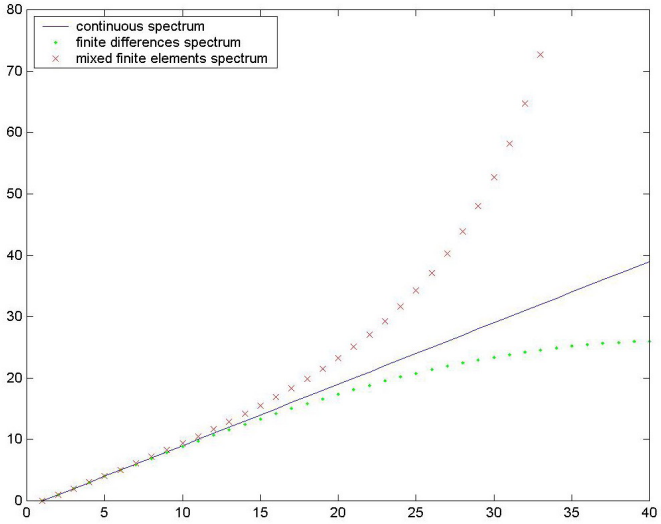

Figure 4.1: $1-D$ Vibration modes of the numerical schemes with finite difference and mixed finite element

Fully-discrete systems

We distinguish two different time discretizations of the previous semi-discrete models: The explicit central difference (EX) and the implicit Newmark scheme with $\gamma = 1/2$ and $\beta = 1/4$ (IM) (see Section 1.4.4).

For a given semi-discrete dispersion relation $\omega = \omega_{sd}(\xi)$ we obtain the following fully-dispersion relations:

1. If we consider the explicit central difference,

$$\omega_{sd}^{ex}(\xi) = \pm\frac{2}{\Delta t}\arcsin\left(\frac{\Delta t}{2}\omega_{sd}(\xi)\right). \tag{4.9}$$

2. If we consider the implicit scheme,

$$\omega_{sd}^{im}(\xi) = \pm\frac{2}{\Delta t}\arcsin\left(\frac{\Delta t}{2}\sqrt{\frac{\omega_{sd}(\xi)^2}{1+\left(\frac{\Delta t}{2}\omega_{sd}(\xi)\right)^2}}\right). \tag{4.10}$$

We analyze the following cases:

1. Assume that we consider a finite difference scheme in space and a central difference scheme in time. Then, the dispersion relation $\omega = \omega_d^{ex}(\xi)$ is given by

$$\omega_d^{ex}(\xi) = \pm\frac{2}{\Delta t}\arcsin\left(\frac{\Delta t}{h}\sin\frac{\xi h}{2}\right). \tag{4.11}$$

When $\Delta t = h$, i.e. $\mu = 1$, we obtain

$$\omega(\xi) = \xi. \tag{4.12}$$

This case is particularly interesting since (4.12) coincides with the dispersion relation for the continuous wave equation. In this case, the discrete waves propagate at a constant velocity identically equal to one, like in the continuous case. But, as we shall see, this is a completely exceptional situation.

When $\mu < 1$, the group velocity is

$$C(\xi,\omega) = \frac{d\omega(\xi)}{d\xi} = \frac{\cos\frac{\xi h}{2}}{\sqrt{1-\left(\frac{\Delta t}{h}\sin\frac{\xi h}{2}\right)^2}}. \tag{4.13}$$

Note that, as $h \to 0$, for all ξ we have

$$C(\xi, \omega) \leq \frac{\cos \frac{\xi h}{2}}{\sqrt{1 - \left(\frac{\Delta t}{h}\right)^2}} \to 0$$

when $\xi \to \pi/h$.

In Figures 1 and Figures 1 we describe the evolution of the group velocity diagrams starting with the semi-discrete case ($\mu = 0$) up to $\mu = 1$, for fixed $h = 0.001$.

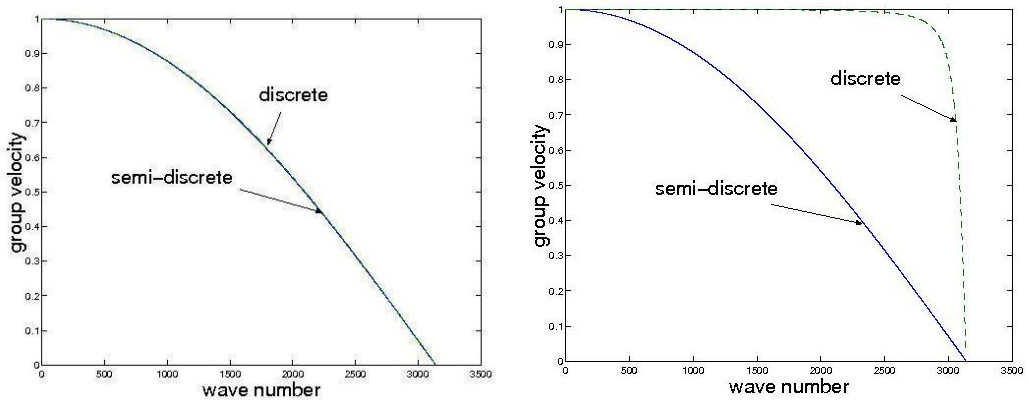

Figure 4.2: Group velocity for the semi-discrete (–) and discrete (- -) cases with $\mu = \Delta t/h = 0.1$ (left),$\mu = \Delta t/h = 0.999$ (right).

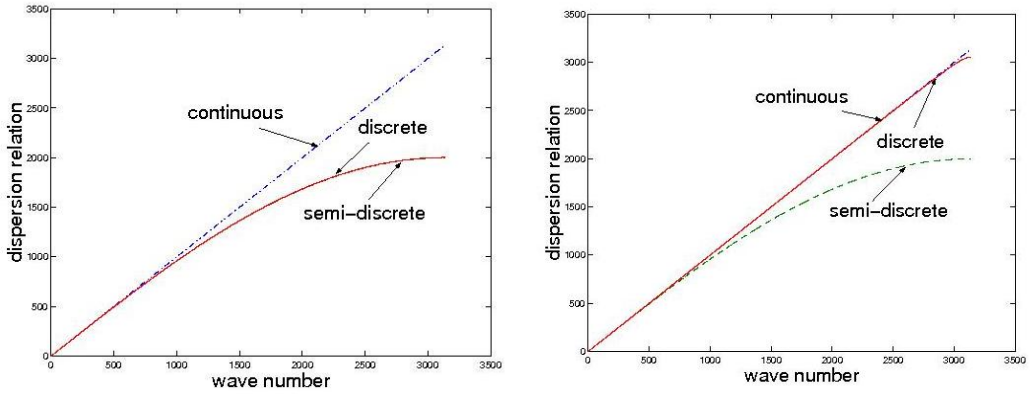

Figure 4.3: Dispersion relation for the continuous (-.-), semi-discrete (- -) and discrete (–) cases with $\mu = \Delta t/h = 0.1$ (left),$\mu = \Delta t/h = 1$ (right).

2. Now we consider a MFE scheme in space and the implicit scheme in time. The dispersion relation is given by

$$\omega_e^{im}(\xi) = \pm \frac{2}{\Delta t} \arcsin\left(\frac{\Delta t}{2} \sqrt{\frac{\omega_e(\xi)^2}{1 + \left(\frac{\Delta t}{2}\omega_e(\xi)\right)^2}}\right). \tag{4.14}$$

A straightforward computation shows that the minimum value of $\omega'(\xi)$ is obtained for $\xi = \pi/h$ and that $\omega'(\pi/h)$ is greater than one if $\Delta t \leq Ch$ for a constant $C > 0$.

4.0.2 $2-D$ numerical schemes for the wave equation

We divide this section in two more subsections where we study the semi-discrete schemes and the fully-discrete ones respectively.

Semi-discrete schemes

We consider two particular space semi-discretization schemes: finite difference (FD) and the mixed finite element scheme (MFE).

For the continuous wave equation, we have $\omega^2(\xi) = |\xi|^2 = |\xi_1|^2 + |\xi_2|^2$ and therefore $c(\xi) = C(\xi) = 1$. In the FD semi-discrete scheme, the dispersion relation is

$$\omega_d^2(\xi) = \frac{4}{h^2}\left(\sin^2\frac{\xi_1 h}{2} + \sin^2\frac{\xi_2 h}{2}\right), \quad \xi \in \left[-\frac{\pi}{h}, \frac{\pi}{h}\right]^2. \tag{4.15}$$

The corresponding group velocity is

$$C(\xi, \omega_d) = \nabla_\xi \omega_d(\xi) = \frac{1}{2\sqrt{\sin^2\frac{\xi_1 h}{2} + \sin^2\frac{\xi_2 h}{2}}}(\sin(\xi_1 h), \sin(\xi_2 h)) \tag{4.16}$$

and it approximates to zero when (ξ_1, ξ_2) tends to $(\pm\pi/h, 0)$ and (ξ_1, ξ_2) tends to $(0, \pm\pi/h)$.

For the MFE semi-discrete scheme, the dispersion relation is

$$\omega_e^2(\xi) = \frac{4}{h^2}\left(\tan^2\frac{\xi_1 h}{2} + \tan^2\frac{\xi_2 h}{2} + \frac{2}{3}\tan^2\frac{\xi_1 h}{2}\tan^2\frac{\xi_2 h}{2}\right), \quad \xi \in \left[-\frac{\pi}{h}, \frac{\pi}{h}\right]^2. \tag{4.17}$$

The corresponding group velocity, $C(\xi, \omega_e) \geq 1$, and tends to infinity when $\xi \approx \pm\pi/h^2$.

In Figure 4.4 we show the dispersion relations of the high vibration modes of the numerical schemes with finite difference and mixed finite element. We have taken $\xi \in [0, 40]^2$. We observe that the dispersion relation associated to the finite differences scheme has some regions where the gradient becomes zero. This is not the case for the continuous and MFE dispersion relations.

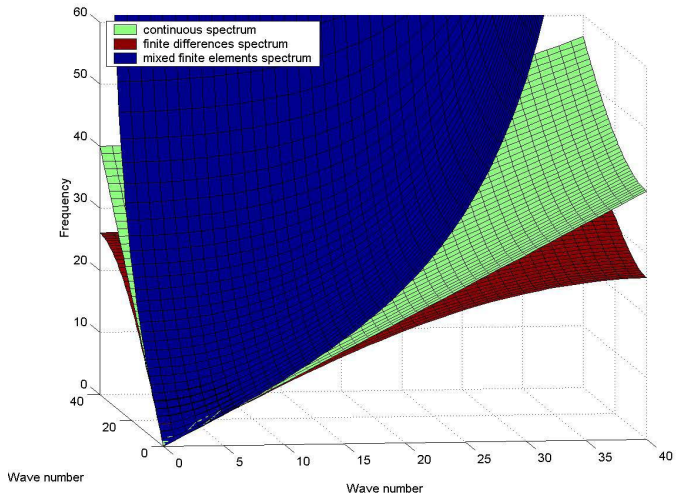

Figure 4.4: $2-d$ dispersion relations of the finite difference approximation (lower surface) continuous wave equation (medium surface) and mixed finite element (upper surface)

Fully-discrete systems

We investigate two different cases

1. Finite differences in space and an explicit scheme in time. The dispersion relation is given by
$$\omega_d^{ex}(\xi) = \pm\frac{2}{\Delta t}\arcsin\left(\frac{\Delta t}{2}\omega_d(\xi)\right). \tag{4.18}$$
The group velocity is
$$C(\xi,\omega) = \nabla_\xi\omega(\xi) = \frac{\nabla_\xi\omega_d(\xi)}{\sqrt{1-\left(\frac{\Delta t}{2}\omega_d(\xi)\right)^2}}. \tag{4.19}$$
Note that, as $h\to 0$, $C(\xi,\omega)$ vanishes when $\xi = (\pi/h, 0)$.

2. MFE scheme in space and implicit in time. Here the dispersion relation is
$$\omega_e^{im}(\xi) = \pm\frac{2}{\Delta t}\arcsin\left(\frac{\Delta t}{2}\sqrt{\frac{\omega_e(\xi)^2}{1+\left(\frac{\Delta t}{2}\omega_e(\xi)\right)^2}}\right). \tag{4.20}$$
A straightforward computation shows that the minimum value of $|\nabla_\xi\omega(\xi)|$ is obtained for $\xi = (\pi/h, \pi/h)$ and that
$$|\nabla_\xi\omega(\pi/h,\pi/h)| \sim h^{3/2}(\Delta t)^{-1}.$$
Therefore, this is uniformly bounded from below if
$$\Delta t = Cte\ h^{3/2}, \quad Cte > 0.$$